Biochemical Pharmacology 81 (2011) 891–909

Contents lists available at ScienceDirect

Biochemical Pharmacology

journal homepage: www.elsevier.com/locate/biochempharm

Taurine suppresses doxorubicin-triggered oxidative stress and cardiac apoptosis in rat via up-regulation of PI3-K/Akt and inhibition of p53, p38-JNK

Joydeep Das, Jyotirmoy Ghosh, Prasenjit Manna, Parames C. Sil *

Division of Molecular Medicine, Bose Institute, P-1/12, CIT Scheme VII M, Kolkata 700054, West Bengal, India

ARTICLE INFO

Article history:
Received 19 November 2010
Received in revised form 21 December 2010
Accepted 18 January 2011
Available online 3 February 2011

Keywords:
Doxorubicin
Cardiac oxidative stress
Reactive oxygen species
p53
NF-κB and MAPK
PI3-K/Akt
Apoptosis
Taurine
Antioxidant
Cell survival

ABSTRACT

The objective of the present study was to investigate the signaling mechanisms involved in the beneficial role of taurine against doxorubicin-induced cardiac oxidative stress. Male rats were administered doxorubicin. Hearts were collected 3 weeks after the last dose of doxorubicin and were analyzed. Doxorubicin administration retarded the growth of the body and the heart and caused injury in the cardiac tissue because of increased oxidative stress. Similar experiments with doxorubicin showed reduced cell viability, increased ROS generation, intracellular Ca^{2+} and DNA fragmentation, disrupted mitochondrial membrane potential and apoptotic cell death in primary cultured neonatal rat cardiomyocytes. Signal transduction studies showed that doxorubicin increased p53, JNK, p38 and NFκB phosphorylation; decreased the levels of phospho ERK and Akt; disturbed the Bcl-2 family protein balance; activated caspase 12, caspase 9 and caspase 3; and induced cleavage of the PARP protein. However, taurine treatment or cardiomyocyte incubation with taurine suppressed all of the adverse effects of doxorubicin. Studies with several inhibitors, including PS-1145 (an IKK inhibitor), SP600125 (a JNK inhibitor), SB203580 (a p38 inhibitor) and LY294002 (a PI3-K/Akt inhibitor), demonstrated that the mechanism of taurine-induced cardio protection involves activation of specific survival signals and PI3-K/Akt as well as the inhibition of p53, JNK, p38 and NFκB. These novel findings suggest that taurine might have clinical implications for the prevention of doxorubicin-induced cardiac oxidative stress.

1. Introduction

Doxorubicin (DOX) is one of the most effective anthracyclin drugs known for the treatment of a variety of cancers, including lymphoma, leukemia, and solid tumors [1,2]. However, some restrictions have been imposed on its clinical use because of profound cardiotoxicity [3,4]. A number of studies have suggested that doxorubicin induces cardiac oxidative stress and cardiotoxicity by reducing myocardial antioxidants [5], perturbing adrenergic function [6], disturbing calcium handling [7] and releasing cardiotoxic cytokines [8]. Several investigators have made efforts to understand the signaling pathways responsible for DOX-induced cardiac apoptosis, although the roles of oxidative stress in the intracellular signaling pathways and apoptosis in this pathophysiology have already been established [9,10].

It is well known that DOX-induced cardiotoxicity occurs via p53-mediated apoptosis [11]. However, some other recent reports have suggested that DOX induces apoptosis in cardiomyocytes via both p53-dependent and p53-independent pathways [12,13]. In the present study, we aimed to investigate the involvement of p53 in DOX-induced cardiac apoptosis. It is also known that nuclear transcription factor kappa B (NF-κB) and mitogen-activated protein kinase (MAPK) signaling pathways are the primary intermediates for the induction of apoptosis by oxidative stress. In the cardiovascular system, extracellular signal-regulated kinase (ERK1/2) is activated by various growth factors and hypertrophic agents that in turn offer cell survival and cytoprotection [14]. c-Jun N-terminal kinases (JNKs) and p38-MAPKs, however, are activated by cellular oxidative stress and correlate with the cardiac pathophysiology and apoptotic cell death [15,16]. Translocation of the NF-κB complex into the nucleus occurs where it can mediate gene transcription in response to cellular activation by extracellular stimuli and regulate the inflammatory response, apoptosis and carcinogenesis. However, depending on the type of cells and the

Abbreviations: CAT, catalase; DOX, doxorubicin; GSH, glutathione; GSSG, glutathione disulfide; GPx, glutathione peroxidase; HDL, high-density lipoprotein; LDH, lactate dehydrogenase; MDA, malondialdehyde; MAPKs, mitogen-activated protein kinases; NF-κB, nuclear factor kappa B; PI3-K, phosphatidylinositol 3-kinase; ROS, reactive oxygen species; SOD, superoxide dismutase; TAU, taurine.

* Corresponding author. Tel.: +91 33 25693243; fax: +91 33 2355-3886.
E-mail addresses: parames@bosemain.boseinst.ac.in, parames_95@yahoo.co.in (P.C. Sil).

0006-2952/$ – see front matter © 2011 Elsevier Inc. All rights reserved.
doi:10.1016/j.bcp.2011.01.008

pathophysiology, NF-κB can either promote or inhibit programmed cell death [17,18]. The literature suggests that DOX induces the activation of both MAPKs and NF-κB in cardiac pathophysiology [19,20]. In the present study, we also investigated the role of MAPKs and NF-κB during DOX-induced myocardium apoptosis in vivo using a rat model and examined whether MAPKs are responsible for the activation of NF-κB and cell death induced by doxorubicin in cardiomyocytes.

The major intracellular free β-amino acid taurine is present in most mammalian tissues and obtained largely from diets [21,22]. It is also known as a conditionally essential amino acid that plays an important role in protecting biological systems from injuries [23–29]. It can attenuate oxidative stress [30], reduce the levels of pro-inflammatory cytokines [31], inhibit apoptosis [32,33] and control blood pressure [34] and calcium homeostasis [35]. Various studies have investigated the protective role of taurine in DOX-induced cardiac pathophysiology. However, little is known about the molecular mechanisms of its protective role in DOX-induced cardiac damage [36,37]. Huang et al. [38] demonstrated decreased cardiac index, left ventricular systolic pressure, SR (Ca^{2+})-ATPase activity and SERCA2a mRNA levels and increased Myo(Ca^{2+}) in DOX-treated rabbits. The authors [38] also showed that taurine supplementation could alleviate the increase in left ventricular diastolic pressure and Myo(Ca^{2+}) and the decrease in SERCA2a mRNA induced by doxorubicin. In the present study, we investigated the signaling mechanisms underlying the protective role of taurine against doxorubicin-induced cardiac apoptosis and oxidative stress using a rat model. We studied the signaling mechanism of the phosphatidylinositol 3-kinase (PI3K)/protein kinase B (Akt) pathways, as these pathways play important roles in the development heart disease and protect cells undergoing apoptosis [39–43]. In this study, we provide evidence for the protective role of anti-apoptotic taurine in doxorubicin-induced cardiotoxicity, which makes this molecule an interesting target for future therapies.

2. Materials and methods

2.1. Chemicals

Taurine (2-aminoethane sulfonic acid), fluo-3, doxorubicin, bovine serum albumin (BSA), Bradford reagent, collagenase type II, Dulbecco's modified Eagle's medium (DMEM), fetal bovine sera (FBS), LY294002, PS-1145, SB203580, SP600125, anti-JNK, anti-p38, anti-ERK, anti-Bcl 2, anti-Bcl XL, anti-caspase 3, anti-Akt and anti-NFkB antibodies were purchased from Sigma–Aldrich Chemical Company (St. Louis, MO, USA). All other antibodies were purchased from Santa Cruz Biotechnology (Santa Cruz, USA). Kits for measurement of LDH, HDL and total cholesterol were purchased from Span diagnostic Ltd., India, and a creatine kinase assay kit was purchased from sigma diagnostics (St Louis, MO, USA). A DNA isolation kit was purchased from G-Bioscience (St Louis, MO, USA). All other chemicals were purchased from Sisco Research Laboratory, India.

2.2. Animals

Four-week old Swiss albino male rats weighing approximately 120–130 g and adult albino Swiss strain mice weighing between 20 and 25 g were purchased from M/S Gosh Enterprises, Kolkata, India. Animals were acclimatized under laboratory conditions for two weeks prior to experiments. All animal experiments were carried out according to the guidelines of the institutional animal ethical committee.

2.3. Determination of dose-dependent activity of taurine by creatine kinase (CK) assay

For this study, rats were randomly distributed into eight groups, each consisting of six animals. The first two groups served as normal controls, which received only water as vehicle, and toxin controls, which received doxorubicin (DOX) in three equal doses (3 mg/kg body weight, i.p. on alternate days). The remaining six groups of animals were treated with six different doses of taurine (50, 75, 100, 150, 200 and 250 mg/kg body weight in distilled water, orally on alternate days) followed by doxorubicin (each injection was given 1 day after taurine).

On day 28 after the first administration of medication (normal saline or doxorubicin), the animals were sacrificed under light ether anesthesia. Blood samples were drawn from the caudal vena cava, collected in test tubes containing heparin solution, and centrifuged at 1500 × *g* for 10 min to obtain serum. CK (creatine kinase) activity in the sera was estimated using standard kits.

2.4. Experimental design for in vivo treatments

The experimental design needed for the present in vivo study is summarized as follows: 6-week-old rats were randomly assigned

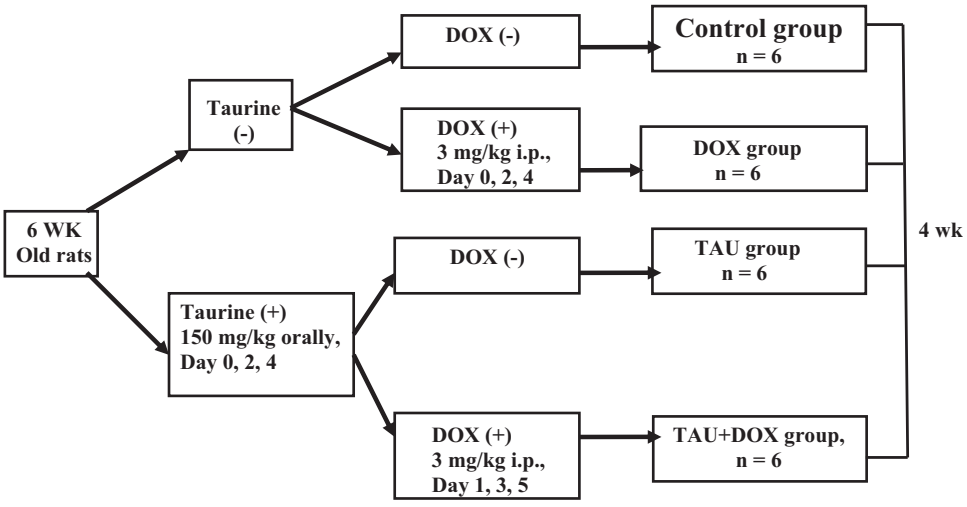

Fig. 1. Schematic diagram of the experimental protocol.

to four groups. Rats in the "control group" received only water as vehicle. Rats in the "DOX group" received doxorubicin (DOX) in three equal doses (3 mg/kg body weight, i.p.) on alternate days for a cumulative dose of 9 mg/kg body weight. This cumulative dose (9 mg/kg) was equivalent to 630 mg for a 70 kg man, just above the threshold at which doxorubicin cardiomyopathy is expected to occur clinically [44]. Rats in the "TAU group" received taurine in three equal doses (150 mg/kg body weight in distilled water, orally) on alternate days for a cumulative dose of 450 mg/kg body weight. Rats in the "TAU + DOX group" received the same dose of taurine as the "Taurine-treated group", followed by a dose of Dox identical to the "DOX group" (each dose was given 1 day after taurine). The study design is summarized in Fig. 1.

On day 28, after the first administration of medication (normal saline, doxorubicin, or taurine), the animals were sacrificed under light ether anesthesia and hearts were collected.

2.5. Determination of heart-to-body weight ratio

After sacrifice, the hearts from experimental animals were quickly excised and weighed. The ratio of heart weight to body weight was then measured for each rat.

2.6. Harvest of serum and cardiac samples

The rats were sacrificed at day 28 after the first administration of medication (normal water, doxorubicin or taurine). The body weight (taken before) and heart weight were measured and compared between groups. Blood samples were drawn from the caudal vena cava, collected in test tubes containing heparin solution, and centrifuged at 1500 × *g* for 10 min to obtain serum. The cardiac tissues were either fixed in 10% formalin for histopathologic examinations or stored at −80 °C until later analysis.

2.7. Preparation of cardiac tissue homogenates

The hearts were minced, washed, and homogenized in a Dounce glass homogenizer in 10 mM HEPES-KOH/1 mM EGTA buffer (pH 7.5) containing 250 mM sucrose and supplemented with protease and phosphatase inhibitors. The homogenates were spun for 10 min at 2000 × *g* to discard the myofilaments at 4 °C. The supernatant was collected and used for the in vivo experiments.- **Determination of protein content**The protein content of the experimental samples was measured using the Bradford method [45] with crystalline BSA as a standard.

2.9. Biochemical analyses

Specific markers related to cardiac dysfunction (e.g., creatine kinase, total cholesterol and HDL cholesterol levels) in the sera were estimated using standard kits. The lipid peroxidation was estimated according to the method of Esterbauer and Cheeseman [46]. LDH activity was determined according to the method of Kornberg [47]. Antioxidant enzyme activity (SOD, CAT, GP_X) and cellular metabolite levels (GSH and GSSG) in the heart tissue were determined following the method described by Das et al. [48].

2.10. Measurement of the cardiac taurine level

The cardiac taurine level was measured according to the method of Ferreira et al. [49]. In brief, sulfosalicylic acid solution was added to the homogenate and allowed to stand for 10 min. It was then filtered through W42 paper and derivatized with o-phthalaldehyde and 2-mercaptcethanol. The derivative was then analyzed by HPLC using a UV absorbance detector at 350 nm.

2.11. Cardiomyocyte isolation and in vitro experimental protocol

Primary cultures of neonatal cardiomyocytes were prepared according to the procedure described by Sil et al. [50]. After 4 days of culture, these preparations contained >95% cardiomyocytes. Cardiomyocytes were then treated with taurine (25 mM), doxorubicin (1 μM) and taurine coupled with doxorubicin (1 h after) for 24 h and were harvested at 4 °C for further molecular and biochemical analyses.

2.12. Assessment of cardiomyocyte viability

Viability of cardiomyocytes was determined using the MTT assay. Briefly, 250 μL of MTT solution (300 mg/mL) was added to the culture medium (200 μL in each well) of cardiomyocytes cultured in 24-well plates 1 h before the end of 24 h treatment and incubated at 37 °C for 30 min. After incubation, supernatants were discarded, and 200 μL of dimethyl sulfoxide was added and mixed thoroughly to dissolve the crystals. Absorbance was measured at 570 nm and 630 nm.

2.13. Measurement of intracellular ROS production

Cardiomyocytes were incubated with DCF-DA (10 mM) for 1 h at 37 °C in the dark. After treatment, the cells were immediately washed and resuspended in PBS. Viable cells incorporated and deacetylated DCFH-DA to 2′,7′-dichlorofluorescin (DCFH), which is not fluorescent. DCFH reacts quantitatively with oxygen species to produce the fluorescent dye 2′,7′-dichlorofluorescein (DCF). Fluorescence emission was measured by flow cytometry using a 525 nm band pass filter, which provides an index of the intracellular oxidative metabolism.

2.14. Flow cytometric and DNA electrophoresis analyses of cardiomyocyte apoptosis

Cardiomyocytes were washed with PBS, centrifuged at 800 × *g* for 6 min, resuspended in ice-cold 70% ethanol/PBS, centrifuged at 800 × *g* for a further 6 min, and resuspended in PBS. Cells were then incubated with propidium iodide (PI) and FITC-labeled Annexin V for 30 min at 37 °C. Excess PI and Annexin V were then washed off; cells were fixed and then analyzed by flow cytometry using a FACS Calibur (Becton Dickinson, Mountain View, CA) equipped with a 488 nm argon laser light source, a 525 nm band pass filter for FITC-fluorescence and a 625 nm band pass filter for PI-fluorescence using CellQuest software. A dot plot of PI fluorescence (*y*-axis) versus FITC fluorescence (*x*-axis) was prepared.

DNA fragmentation was also assayed by electrophoresing genomic DNA samples isolated from normal and experimental rat hearts, as above, on an agarose gel containing ethidium bromide by the procedure described by Sellins and Cohen [51].

2.15. Isolation of mitochondria and determination of mitochondrial membrane potential ($\Delta\psi_m$)

Mitochondria were isolated from the cardiomyocytes. The cardiomyocytes were isolated in 10 mL buffer containing 0.1 M Tris–Mops, pH 7.4, 20 mL 1 M sucrose, and 1 mL 0.1 M EGTA–Tris buffer, pH 7.4. The cardiomyocytes were then sonicated and centrifuged at 800 × *g* for 10 min at 4 °C, and the supernatant was collected and centrifuged for 30 min at 10,000 × *g*. The supernatant was then discarded, and the mitochondria pellet were resuspended in the same buffer and recentrifuged for 10 min at 10,000 × *g*. This supernatant was also discarded, and the final mitochondrial pellet was resuspended in PBS. It was stored at −80 °C until use. Analytic flow cytometric measurements for the

membrane potential ($\Delta\psi_m$) of isolated mitochondria were performed using a FACScan flow cytometer with an argon laser excitation at 488 nm and a 525 nm band pass filter. The mitochondrial membrane potential ($\Delta\psi_m$) was estimated on the basis of cell retention of the fluorescent cationic probe rhodamine 123.

2.16. Measurement of intracellular free Ca^{2+}

Intracellular Ca^{2+} levels were determined using the intracellular Ca^{2+} probe Fluo 3/acetoxymethyl ester (Molecular Probes, Inc.), which binds Ca^{2+} with a 1:1 stoichiometry. Cardiomyocytes were incubated in the dark with 250 nM Fluo-3 for 30 min at 37 °C. Fluorescence was measured on FL1 (530 nm) in a BD Biosciences FACScan flow cytometer with excitation at 488 nm, and CellQuest software was employed for subsequent data analysis.

2.17. Preparation of cytosolic and nuclear extracts from cardiomyocytes

Nuclear and cytosolic proteins were extracted from cardiomyocytes according to the procedure described by Goren et al. [52]. This nuclear extract was subjected to immunoblotting analysis to determine the protein expression of NF-κB in vitro.

2.18. Immunoblotting

An equal amount of protein (50 μg) from each sample was resolved by 10% SDS-PAGE and transferred to a PVDF membrane. Membranes were blocked at room temperature for 2 h in blocking buffer containing 5% non-fat dry milk to prevent nonspecific binding and were then incubated with anti-p-53 (1:1000 dilution), anti-phospho and anti-total p-38 (1:1000 dilution), anti-phospho and anti-total ERK1/2 (1:1000 dilution), anti-phospho and anti-total p-JNK (1:1000 dilution), anti-phospho and anti-total NF-κB (p65) (1:250 dilution), anti-phospho and anti-total IKK-α/β (1:1000 dilution), anti-phospho and anti-unphospho Iκ≡-α (1:1000 dilution), anti-Bad (1:1000 dilution), anti-Bax (1:1000 dilution), anti-Bcl-2 (1:1000 dilution), anti-Bcl-xL (1:1000 dilution), anti-cytochrome c (1:1000 dilution), anti-caspase 9 (1:1000 dilution), anti-caspase 3 (1:1000 dilution), anti-caspase 12 (1:1000 dilution), anti-PARP (1:1000 dilution), anti-Akt (1:100 dilution) and anti-PI3-K (1:100 dilution) primary antibodies separately at 4 °C overnight. The membranes were washed in TBST (50 mmol/L Tris–HCl, pH 7.6, 150 mmol/L NaCl, 0.1% Tween 20) for 30 min, incubated with the appropriate HRP-conjugated secondary antibody (1:2000 dilution) for 2 h at room temperature and developed by the HRP substrate 3,3′-diaminobenzidine tetrahydrochloride (DAB) system (Bangalore Genei, India).

2.19. Histological studies

Hearts from the normal and experimental rats were fixed in 10% buffered formalin and were processed for paraffin sectioning. Sections of approximately 5 μm thickness were stained with hematoxylin and eosin to study the heart histology of all experimental rats.

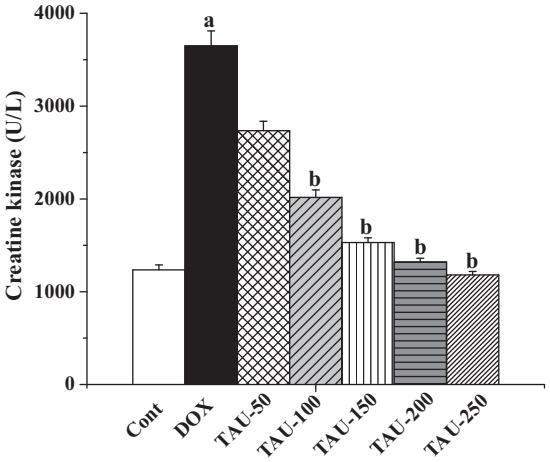

Fig. 2. Dose dependent effect of taurine on CK activities. Cont: CK activity in normal rats; DOX: CK activity in rats received doxorubicin (DOX) in three equal doses (3 mg/kg body weight, i.p.) on alternate days; TAU-50, TAU-100, TAU-150, TAU-200 and TAU-250: CK activities in rats received taurine in three equal doses (50, 100, 150, 200 and 250 mg/kg body weight respectively in distilled water, orally) on alternate days followed by DOX exposure. Each column represents mean ± SD, $n = 6$. "*a*" indicates the significant difference between the control and DOX-exposed groups and "*b*" indicates the significant difference between TAU + DOX treated and DOX-exposed groups. ($P^a < 0.05$, $P^b < 0.05$).

2.20. Statistical analysis

All the values are expressed as mean ± S.D. ($n = 6$). Significant differences between the groups were determined with SPSS 10.0 software (SPSS Inc., Chicago, IL, USA) for Windows using a one-way analysis of variance (ANOVA), and the group means were compared by Duncan's Multiple Range Test (DMRT). A difference was considered significant at the $P < 0.05$ level.

3. Results

3.1. Dose-dependent study of taurine by CK assay

Creatine kinase (CK) was assayed to determine the optimum dose necessary for taurine to protect the rat heart against DOX-induced cardio-toxicity. The results suggest that DOX intoxication (3 mg/kg body weight, i.p. on alternate days) increased the serum CK activity, but it could be prevented by taurine treatment up to a dose of 150 mg/kg body weight in distilled water, orally, 1 day before each dose of doxorubicin (Fig. 2). However, a higher dose of taurine provided no additional benefit to serum CK activity, and so 150 mg/kg body weight taurine was selected for subsequent in vivo experiments.

3.2. Suppression of the deleterious effects of doxorubicin by taurine on the body and heart growth

During treatment, all animals appeared lively and no mortality was encountered in either of the groups. Among the four groups of

Table 1
Effect of doxorubicin and taurine on the heart and body weight of experimental animals.

Name of the parameters	Control group	DOX group	TAU + DOX group	TAU group
Body weight(g)	174.0 ± 6.71	142.6 ± 5.13	168.0 ± 6.14	178.8 ± 6.29
Heart weight(g)	1.28 ± 0.04	1.10 ± 0.03	1.24 ± 0.05	1.30 ± 0.05
Ratio of the heart weight to the body weight (%)	0.736 ± 0.02	0.771 ± 0.03	0.738 ± 0.02	0.727 ± 0.02

Values are expressed as mean ± SD, for 6 animals in each group.

Table 2
Effect of doxorubicin and taurine on the levels of the serum markers related to cardiac dysfunction.

Name of the parameters	Control group	DOX group	TAU + DOX group	TAU group
CK (U/L)	1235 ± 20.75	3649 ± 48.42[a]	1530 ± 21.51[b]	1186 ± 20.15
Total cholesterol (mg/dL)	98.51 ± 2.35	192.42 ± 5.73[a]	116.46 ± 3.48[b]	102.62 ± 2.82
HDL cholesterol (mg/dL)	22.09 ± 0.87	14.06 ± 0.41[a]	20.62 ± 0.72[b]	21.48 ± 0.81
LDH (U/L)	206.3 ± 6.31	323.8 ± 8.27[a]	254.9 ± 7.58[b]	198.5 ± 6.21

Values are expressed as mean ± SD, for 6 animals in each group. "*a*" values differ significantly from control ($P^a < 0.05$); "*b*" values differ significantly from DOX ($P^b < 0.05$).

Table 3
Effect of doxorubicin and taurine on the status of the thiol based antioxidants and lipid peroxidation.

Name of the parameters	Control group	DOX group	TAU + DOX group	TAU group
MDA (nmol/mg protein)	1.62 ± 0.04	4.27 ± 0.18[a]	2.41 ± 0.11[b]	1.27 ± 0.03
GSH (nmol/mg protein)	18.96 ± 0.57	13.12 ± 0.46[a]	16.48 ± 0.49[b]	19.68 ± 0.59
Redox ratio (GSH/GSSG)	46.06 ± 1.53	7.56 ± 0.27[a]	36.27 ± 1.19[b]	48.94 ± 1.57

Values are expressed as mean ± SD, for 6 animals in each group. "*a*" values differ significantly from control ($P^a < 0.05$); "*b*" values differs significantly from DOX ($P^b < 0.05$).

animals, the DOX group had gained less body weight and heart weight compared with those in the control group at 28 days. However, treatment with taurine increased the body and heart weight compared with doxorubicin-treated rats, demonstrating the growth-impeding effect of doxorubicin and the counteracting action of taurine against doxorubicin (Table 1). Conversely, the relative heart weight index (heart weight to body weight ratio) was similar among all four groups at 28 days (Table 1).

3.3. Taurine attenuated cardiotoxicity and oxidative stress induced by doxorubicin

In the present study, doxorubicin induced severe biochemical changes and oxidative damage in the heart tissues. Myocardial damage in the DOX group was assessed by measuring total and HDL cholesterol, LDH and CK activity. DOX exposure significantly increased total cholesterol and LDH levels and CK activity, but it decreased HDL cholesterol level (Table 2). Treatment with taurine, however, maintained these levels near baseline (Table 2).

Doxorubicin is a potential source of ROS. The formation of ROS is considered the rate-limiting step in lipid peroxidation. The biochemical determination of malondialdehyde (MDA) indicates lipid peroxide formation. We observed that DOX significantly increased the MDA level in heart tissue compared with the normal group (Table 3). However, treatment with taurine significantly reduced this level (Table 3).

Increased oxidative stress decreases intracellular GSH and increases the formation of GSSG, thereby leading to imbalance in the GSH/GSSG redox couple. In the present study, DOX treatment significantly reduced the cardiac GSH level and the GSH/GSSG ratio (Table 3). Treatment with taurine, however, maintained these levels near baseline (Table 3).

Anti-oxidant enzyme activities (SOD, CAT, GPx) reflect the level of oxidative stress of the tissue examined. The anti-oxidant enzyme activities in the hearts of all groups of rats are illustrated in Table 4. Compared with the control groups, doxorubicin-exposed hearts possessed significantly less anti-oxidant enzyme activity, whereas taurine treatment effectively prevented doxorubicin-induced reduction of anti-oxidant enzyme activity.

3.4. Effect of doxorubicin on the cardiac taurine level

Table 5 shows the level of taurine in the heart tissue of DOX-exposed animals. Doxorubicin administration caused a significant reduction in the taurine level in cardiac tissues, but it was significantly prevented by taurine treatment. Conversely, the

Table 4
Effect of doxorubicin and taurine on the activities of the antioxidant enzymes in cardiac tissue.

Name of the parameters	Control group	DOX group	TAU + DOX group	TAU group
SOD (Unit/mg protein)	98.20 ± 2.91	47.48 ± 1.27[a]	87.24 ± 2.48[b]	98.22 ± 3.27
CAT (μmol/min/mg protein)	52.21 ± 1.61	29.80 ± 1.21[a]	49.02 ± 1.58[b]	51.17 ± 1.59
GPx (nmol/min/mg protein)	139.49 ± 4.28	87.14 ± 2.35[a]	121.43 ± 4.07[b]	141.2 ± 4.08

Values are expressed as mean ± SD, for 6 animals in each group. "*a*" values differ significantly from control ($P^a < 0.05$); "*b*" values differs significantly from DOX ($P^b < 0.05$).

Table 5
Taurine concentration in the heart tissues of experimental animals.

Name of the parameter	Control group	DOX group	TAU+DOX group	TAU group
Taurine (μmol/g tissue)	30.21 ± 1.05	19.5 ± 0.48[a]	25.3 ± 0.89[b,c,d]	38.8 ± 1.09

Values are expressed as mean ± SD, for 6 animals in each group. "*a*" values differs significantly from control ($P^a < 0.05$); "*b*" values differs significantly from DOX ($P^b < 0.05$). "*c*" values indicate significant difference between TAU + DOX and control ($P^c < 0.05$); "*d*" values differs significantly from TAU ($P^d < 0.05$).

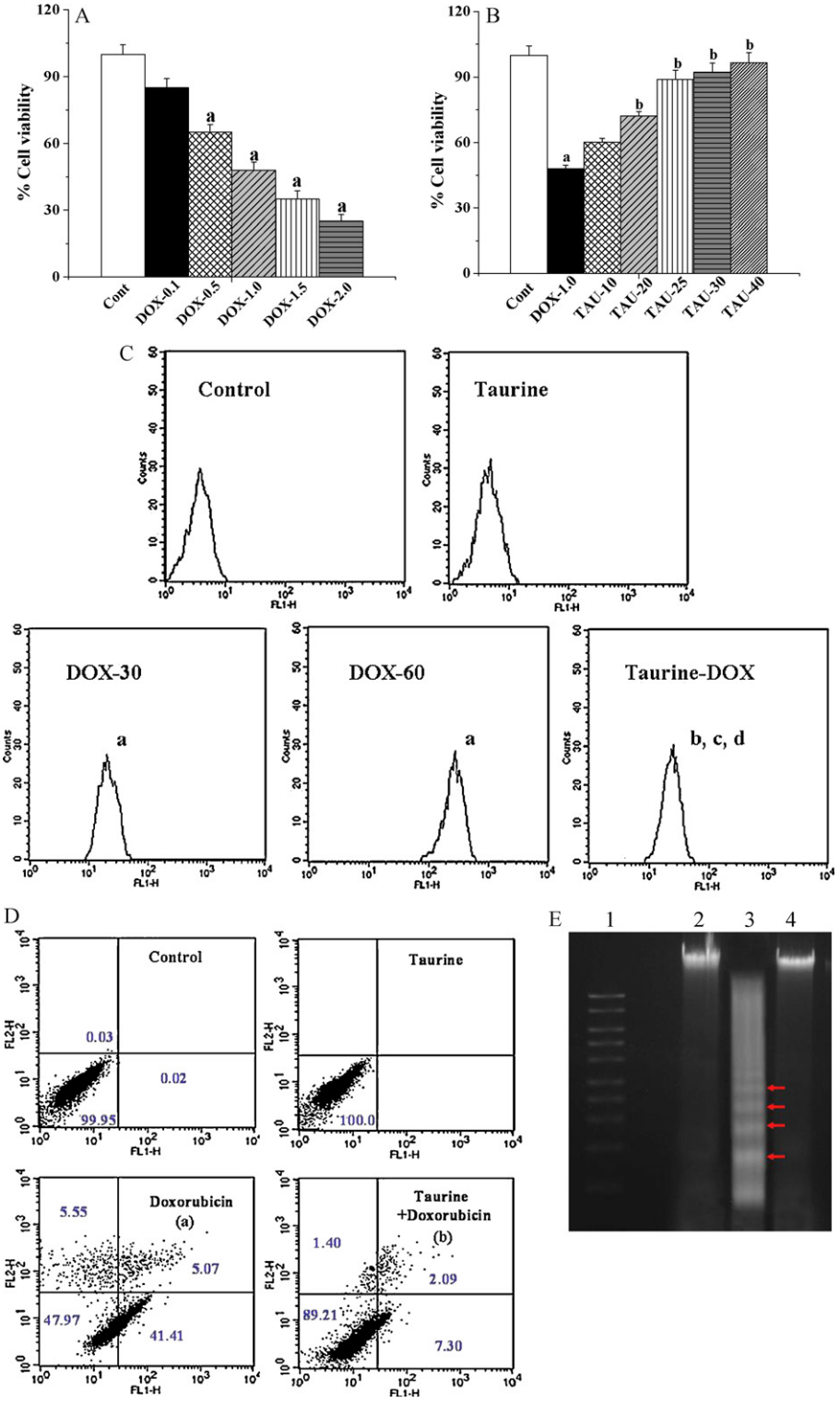

Fig. 3. (A and B) Impact of DOX and taurine on cell viability, ROS production, mode of cell death and $\Delta\psi_m$ in cardiomyocytes. Panel A: dose dependent effect of DOX on cell viability; Panel B: dose dependent effect of taurine on DOX-exposed cardiomyocytes; Cont: cell viability in normal cardiomyocytes; DOX-0.1, DOX-0.5, DOX-1.0, DOX-1.5 and DOX-2.0; cell viability in DOX-exposed cardiomyocytes for 8 h at a dose of 0.1, 0.5, 1.0, 1.5 and 2 μM; TAU-10, TAU-20, TAU-25, TAU-30, and TAU-40: cell viability level in cardiomyocytes treated with taurine (1 h prior to DOX addition) and DOX for 24 h at a dose of 10, 20, 25, 30 and 40 mM. "*a*" indicates the significant difference between the control and DOX-treated cells, "*b*" indicates the significant difference between DOX and taurine-DOX treated cells. Each column represents mean ± SD, $n = 6$; ($P^a < 0.05$, $P^b < 0.05$). (C–F) Impact of DOX and taurine on ROS production, mode of cell death and $\Delta\psi_m$ in cardiomyocytes. Panel C: the intracellular ROS production was detected by flow cytometer. Cont: ROS production in normal cardiomyocytes. DOX-30, DOX-60: ROS production in DOX-exposed cardiomyocytes after 30 and 60 min of intoxication. Results represent one of the six independent experiments. Panel D: percent distribution of apoptotic and necrotic cells using flow cytometer. Results expressed as dot plot representing as one of the six independent experiments. Panel E: DNA fragmentation pattern on agarose/EtBr gel. Lane 1: Marker (1 kb DNA ladder); Lane 2, Lane 3, Lane 4: DNA isolated from normal, DOX intoxicated and taurine treated cardiomyocytes respectively. Arrows indicate ladder formation. Panel F: mitochondrial membrane potential ($\Delta\psi_m$) was measured using flow cytometer with FL-1 filter. Results represent one of the six independent experiments. "*a*" indicates the significant difference between the control and DOX-treated cells. "*b*" indicates the significant difference between DOX and TAU + DOX treated cells. "*c*" indicates the significant difference between the control and TAU + DOX treated cells. "*d*" indicates the significant difference between TAU and TAU + DOX treated cells. ($P^a < 0.05$, $P^b < 0.05$, $P^c < 0.05$, $P^d < 0.05$).

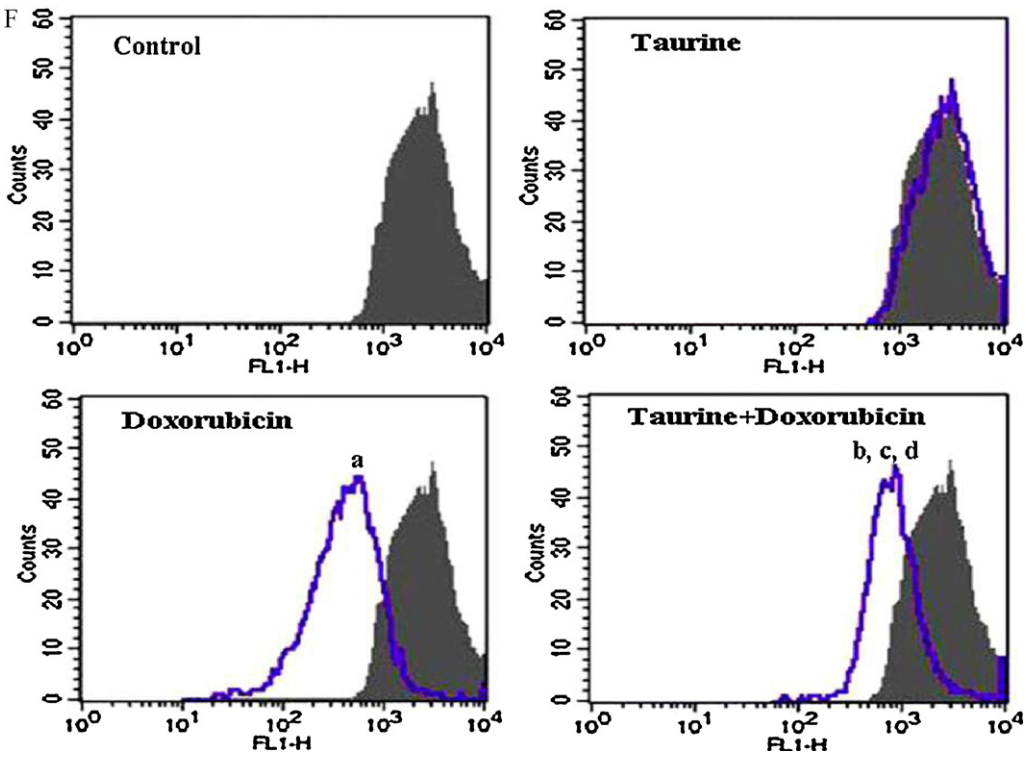

Fig. 3. (*Continued*).

taurine level was lower in taurine-DOX treated animals compared with the animals treated with taurine alone.

3.5. Taurine protected against doxorubicin-induced cytotoxicity and apoptosis

To determine the effects of DOX on the viability of cardiomyocytes, the cells were treated with various concentrations (0.1–2 μM) of DOX and the viable cell numbers were estimated using the MTT assay. DOX reduced the number of viable cardiomyocytes in a concentration-dependent manner (Fig. 3A). DOX, at the 1 μM dose, reduced cell viability to 50% compared with untreated cardiomyocytes. Therefore, this dose of DOX was selected for the subsequent in vitro studies. However, cardiomyocyte treatment with increasing concentrations of taurine dose-dependently suppressed DOX-induced reductions in cell viability. Treatment with 25 mM taurine was found to be effective in preventing DOX-induced (1 μM) reductions in cell viability (Fig. 3B). Taurine in the absence of DOX exerted no effect on the cardiomyocyte viability.

After 30 min of DOX intoxication, we observed that production of intracellular reactive oxygen species (ROS) was increased and this level was further increased at 1 h. By itself, taurine treatment of the cardiomyocytes did not show any effect on ROS levels (Fig. 3C). However, the DOX-induced increase in ROS production was significantly mitigated by taurine treatment.

To estimate the number of apoptotic cells, the cells were stained with annexin V and propidium iodide and were then analyzed via flow cytometry. We observed a significant increase in apoptotic cell numbers in the DOX-treated cardiomyocytes. The treatment of cells with taurine, however, mitigated this effect. Taurine alone exerted no effect on apoptosis in cardiomyocytes (Fig. 3D).

We next examined the DNA fragmentation pattern to show the apoptotic changes in the cardiomyocytes. DOX caused a DNA ladder fragmentation (a hallmark of apoptosis) (Fig. 3E). Taurine treatment effectively reduced the DNA laddering in the DOX-treated cardiomyocytes.

3.6. Taurine suppressed doxorubicin-induced disruption of mitochondrial membrane potential ($\Delta\psi_m$)

Maintenance of intact mitochondrial membrane potential ($\Delta\psi_m$) is fundamental to cell survival, and the loss of ($\Delta\psi_m$) triggers a cascade of reactions leading to cell apoptosis. To determine whether doxorubicin induced apoptosis through disrupting $\Delta\psi_m$ while taurine sustained it, $\Delta\psi_m$ was measured using flow cytometry. We observed that DOX exposure significantly reduced $\Delta\psi_m$ in mitochondria isolated from the rat heart, whereas taurine treatment increased $\Delta\psi_m$, confirming the disruptive effect of doxorubicin and the preservative effect of taurine on mitochondrial $\Delta\psi_m$ (Fig. 3F).

3.7. Taurine inhibited DOX-induced intrinsic apoptotic pathways in cardiomyocytes and heart

As taurine suppressed DOX-induced apoptosis, we assessed the effects of DOX and taurine on the levels of Bcl-2 family proteins, mitochondrial cytochrome c release and DOX-induced cleavage of caspases and PARP in cardiomyocytes and rat hearts. Immunoblotting studies demonstrated that doxorubicin down-regulated the anti-apoptotic (Bcl-2, Bcl-xL) and up-regulated the pro-apoptotic (Bax, Bad) Bcl-2 proteins in cardiomyocytes and in heart tissue (Fig. 4A–D), whereas taurine treatment effectively repressed these doxorubicin-evoked pro-apoptotic events.

Cytochrome c is located in the mitochondrial intermembrane space in the resting state. Stimuli that disrupt mitochondrial

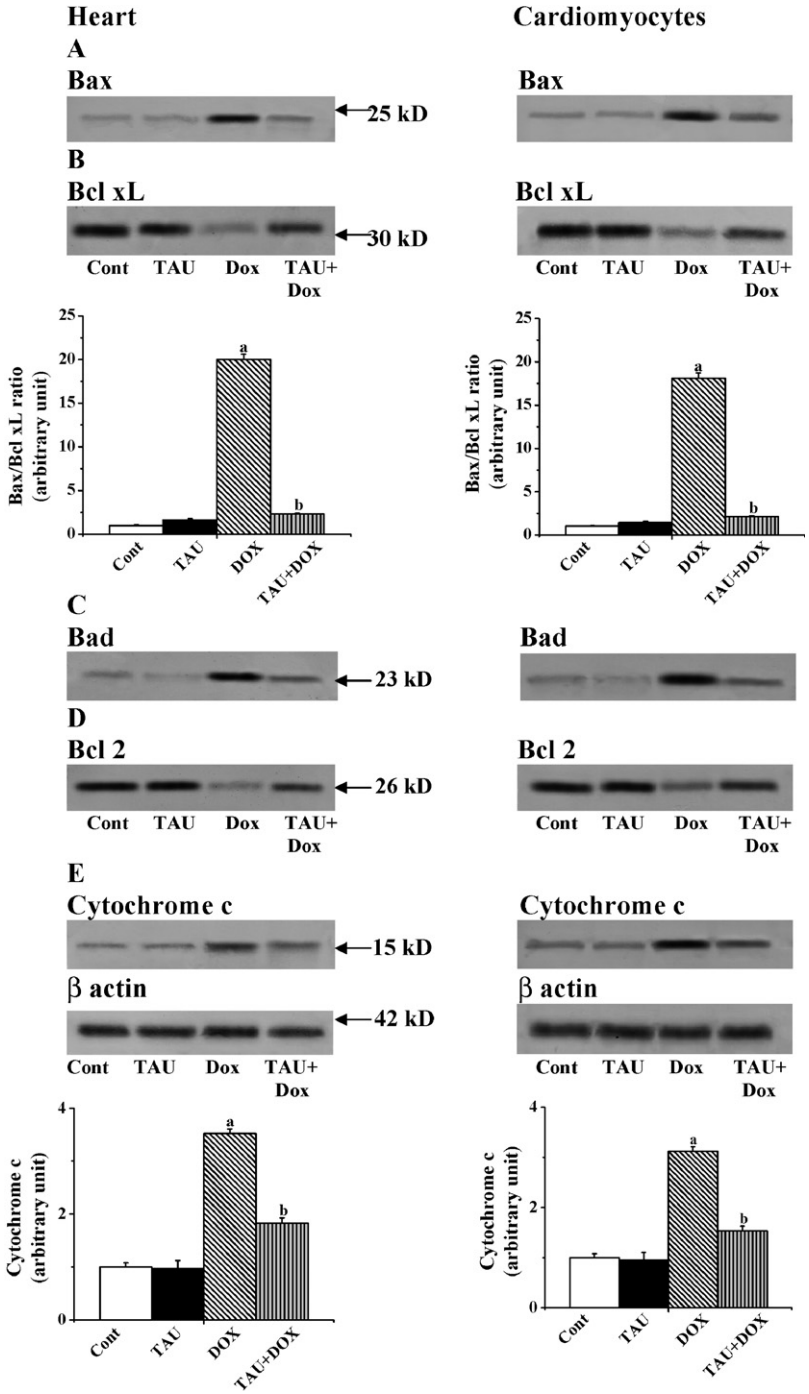

Fig. 4. Immunoblot analysis on mitochondrion-dependent pathway in absence (DOX) and presence of taurine (TAU + DOX) in both heart and cardiomyocytes. Panel A: Bax, Panel B: Bcl-xL, Panel C: Bad, Panel D: Bcl-2, Panel E: cytosolic cytochrome c. β actin was used as an internal control. Data represent the average ± SD of 6 separate experiments in each group. "*a*" indicates the significant difference between the control and DOX-exposed groups, "*b*" indicates the significant difference between the DOX treated and taurine treated groups.($P^a < 0.05$, $P^b < 0.05$).

potential ($\Delta\psi_m$) induce cytochrome c release from mitochondria to the cytosol and trigger downstream cell signaling events that lead to apoptosis. The immunoblotting study demonstrated that cytosolic cytochrome c abundance increased in doxorubicin-treated cardiomyocytes (Fig. 4E) but remained practically unaltered when treated with taurine. These findings indicate that taurine treatment can counteract doxorubicin-triggered cytochrome c release in cardiomyocytes.

Cardiomyocyte apoptosis was also studied in terms of caspase-3 activation and PARP cleavage. Treatment of the cardiomyocytes with DOX resulted in a marked increase in the levels of cleaved caspase-9 and caspase 3 at 6 h, and taurine inhibited these effects (Fig. 5A and B). Cleaved PARP levels were increased dramatically by DOX treatment, and this effect was also significantly inhibited by taurine treatment (Fig. 5C).

3.8. Taurine attenuated the doxorubicin-induced increase in intracellular Ca^{2+} and the sarcoplasmic reticulum-mediated apoptotic pathway

To investigate the involvement of the ER/SR-mediated pathway of apoptosis, we analyzed the intracellular Ca^{2+}

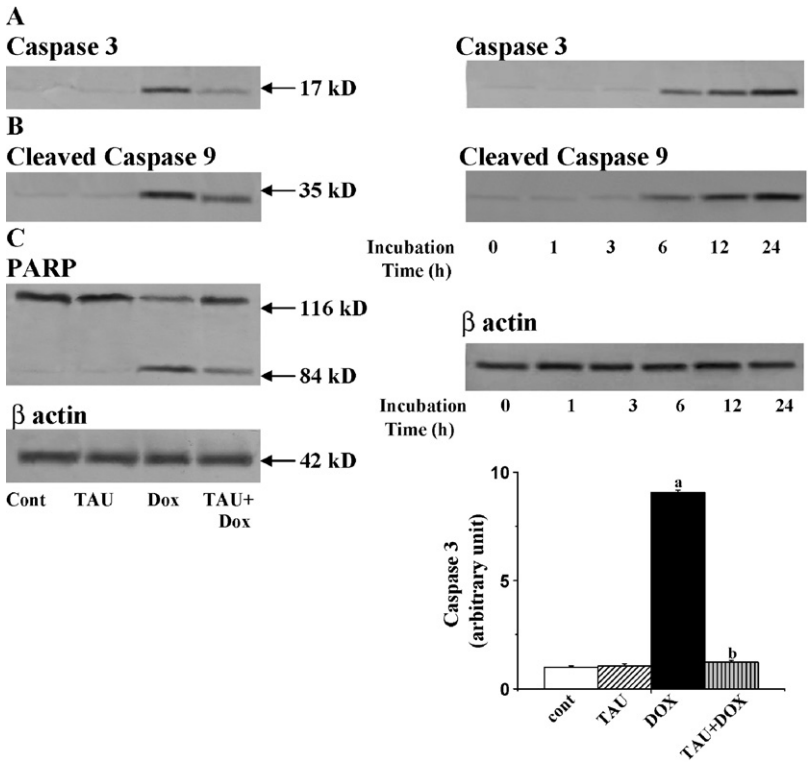

Fig. 5. Immunoblot analysis of caspases 3, 9 and PARP in absence (DOX) and presence of taurine (TAU + DOX) in cardiomyocytes. Panel A: time dependent effect on caspase 3 activation after DOX exposure in cardiomyocytes, Panel B: time dependent effect on caspase 9 activation after DOX exposure in cardiomyocytes, Panel C: PARP. β actin was used as an internal control. Data represent the average ± SD of 6 separate experiments in each group. "*a*" indicates the significant difference between the control and DOX-exposed groups, "*b*" indicates the significant difference between the DOX treated and taurine treated groups (TAU + As).($P^a < 0.05$, $P^b < 0.05$).

level and caspase-12 expression because increased intracellular Ca^{2+} concentrations significantly increase susceptibility to apoptosis via activation of caspase-12. As depicted in the histogram in Fig. 6A, cardiomyocytes exposed to DOX had increased FL1 fluorescence, indicating an increased concentration of intracellular Ca^{2+} after 30 min of DOX exposure. Intracellular Ca^{2+} was further increased after 1 h of DOX exposure. DOX exposure also significantly increased the cellular level of caspase-12 (Fig. 6B), indicating the involvement of ER/SR-mediated apoptosis. However, taurine treatment could reduce these intracellular Ca^{2+} concentrations and caspase-12 activation.

3.9. Taurine repressed the DOX-induced activation of p53

To delineate the signaling pathway of DOX-induced apoptosis, cellular p53 expression was examined. The expression of p53 was markedly up-regulated in the hearts and cardiomyocytes exposed to DOX (Fig. 7). However, treatment with taurine could counteract this DOX-induced alteration.

3.10. Phosphorylation of IKKα, IKKβ, NFκB and IκBα

In the present study to investigate the pro-apoptotic effect of NF-κB in DOX-induced myocardial injury, we examined the phosphorylation of IKKα, IKKβ, NF-κB and Iκ≡α The phosphorylation pattern of Iκ≡α, IKKα, IKKβ and NFκ≡ was examined in the cardiomyocytes exposed to DOX, taurine, and taurine + DOX. DOX exposure caused a significant increase in Iκ≡α, IKKα, IKKβ and NFκB phosporylation and a decrease in unphosphorylated Iκ≡α compared with the respective control group after 24 h (Fig. 8A–C). As shown in Fig. 8C, the expression of phospho NF-κB increased with time in DOX-treated cardiomyocytes, beginning at 3 h of incubation. Taurine treatment alone did not cause any change in these parameters, whereas the DOX-induced increase in IKKα, IKKβ, NFκB and Iκ≡α phosphorylation was prevented by taurine treatment (Fig. 8A–C).

3.11. Inhibition of DOX-induced apoptosis by an NFκB inhibitor

To investigate the role of NFκB in the DOX-induced cellular response, we used the IKK inhibitor PS-1145. Cardiomyocytes were pre-incubated with PS-1145 (25 μM) for 15 min followed by DOX exposure (1 μM for 24 h). Cardiomyocyte apoptosis was studied by evaluating caspase-3 activation and PARP cleavage after inhibiting IKK with PS-1145. PS-1145 dramatically blocked DOX-induced caspase-3 activation and PARP cleavage (Fig. 9A and B). These results confirm that NFκB activation functions as a pro-apoptotic factor in DOX-induced cardiomyocyte apoptosis.

3.12. Phosphorylation of different MAPKs in doxorubicin-induced cardiac pathophysiology

Phosphorylation of ERK1/2, p38, and JNK kinases was examined in the hearts and cardiomyocytes of the control, DOX, taurine + -DOX and taurine groups, and the immunoblotting data are shown in Fig. 10A–D. Phosphorylation of ERK1/2 was significantly reduced in the DOX group compared with the control group in both rat hearts (after 28 days) and cardiomyocytes (after 24 h incubation), and taurine could not prevent this decrease (Fig. 10A). By contrast, as shown in Fig. 10B–C, phosphorylation of both JNK and p38 was significantly increased in the DOX group compared with the control group in both rat hearts (after 28 days) and cardiomyocytes

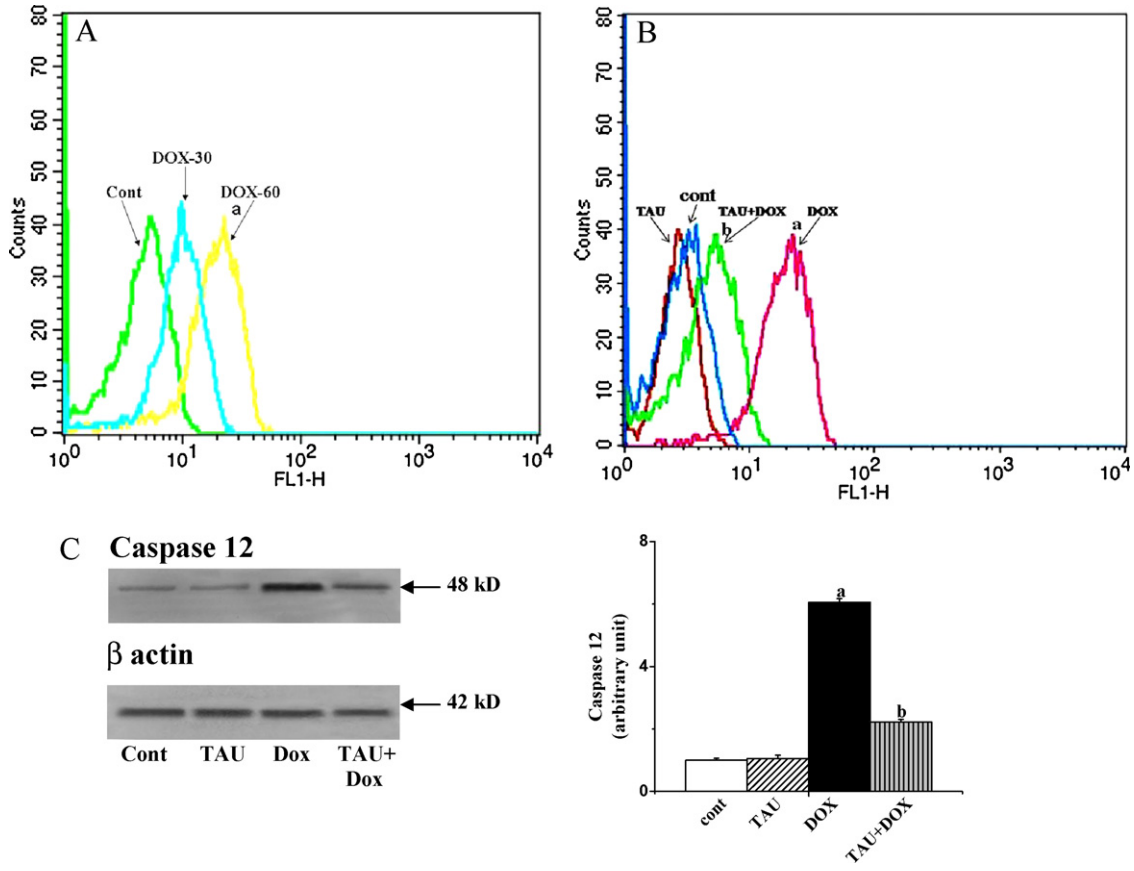

Fig. 6. Investigation of sarcoplasmic reticulum-mediated pathway in absence (DOX) and presence of taurine (TAU + DOX) in cardiomyocytes. Panel A: intracellular Ca^{2+} levels were monitored at 30 and 60 min after DOX administration by flow cytometer. Panel B: intracellular Ca^{2+} level after 60 min of DOX administration and effect of taurine. Results represent one of the six independent experiments. Panel C: protein level of caspase 12, β actin was used as an internal control. Data represent the average ± SD of 6 separate experiments in each group. "*a*" indicates the significant difference between the control and DOX-exposed groups, "*b*" indicates the significant difference between the DOX treated and taurine treated groups.($P^a < 0.05$, $P^b < 0.05$).

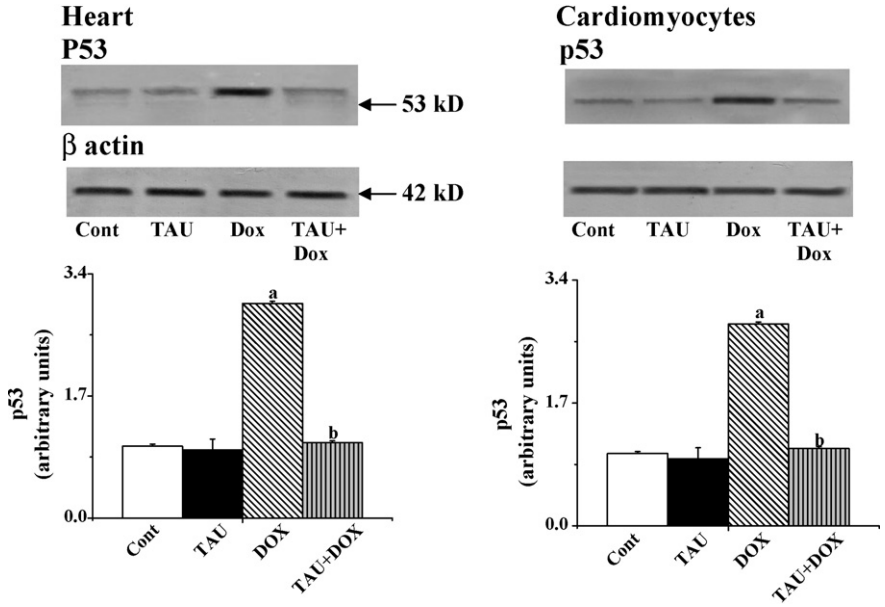

Fig. 7. Investigation of the involvement of p53 in response to DOX and taurine (TAU + DOX) in rat hearts and cardiomyocytes. β actin was used as an internal control. Data represent the average ± SD of 6 separate experiments in each group. "*a*" indicates the significant difference between the control and DOX-exposed groups, "*b*" indicates the significant difference between the DOX treated and taurine treated groups.($P^a < 0.05$, $P^b < 0.05$).

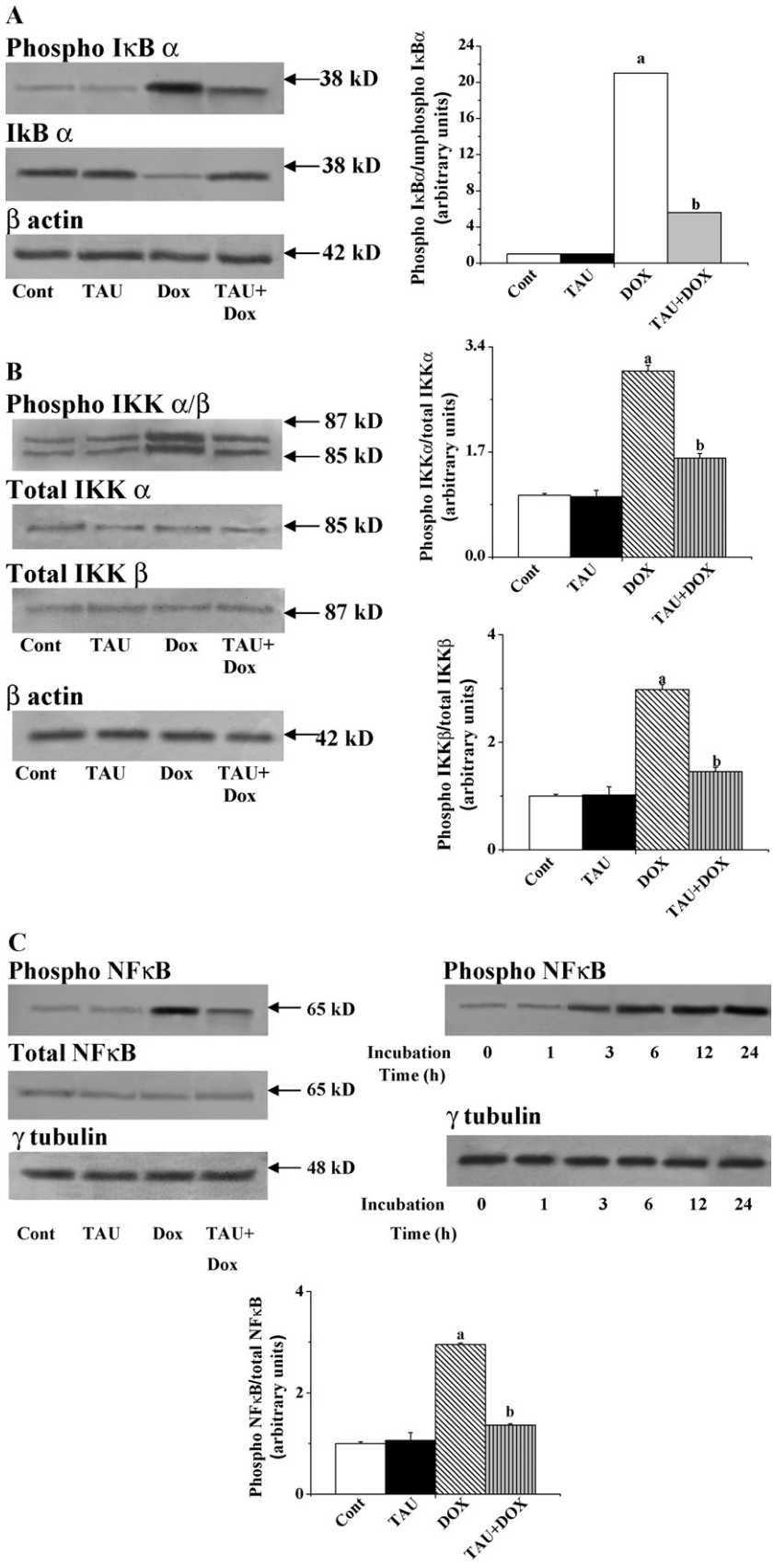

Fig. 8. Immunoblot analysis of IKKα/β, NFκB and IκBα proteins in response to DOX and taurine (TAU + DOX). Panel A: phospho and unphospho IκBα. β actin was used as an internal control. Panel B: phospho and total IKKα/β, β actin was used as an internal control. Panel C: phospho and total NFκB as well as time dependent effect on NFκB activation, γ tubulin was used as an internal control. Data represent the average ± SD of 6 separate experiments in each group. "*a*" indicates the significant difference between the control and DOX-exposed groups, "*b*" indicates the significant difference between the DOX treated and taurine treated groups.($P^a < 0.05$, $P^b < 0.05$).

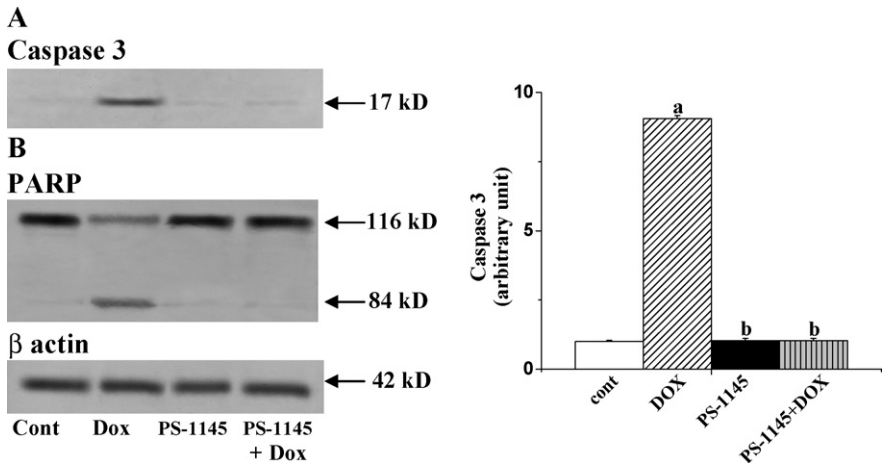

Fig. 9. Immunoblot analysis of IKKα/β, NFκB, caspase 3 and PARP in cardiomyocytes in response to PS-1145. Cardiomyocytes were pre-treated with 25 μM PS-1145 for 15 min, then treated with DOX (1 μM) for 24 h. Panel A: phospho NFκB, γ tubulin was used as an internal control. Panel B: phospho IKKα/β, Panel C: caspase 3, Panel D: PARP. β actin was used as an internal control. Data represent the average ± SD of 6 separate experiments in each group. "*a*" indicates the significant difference between the control and DOX-exposed groups, "*b*" indicates the significant difference between the DOX treated and taurine treated groups.($P^a < 0.05$, $P^b < 0.05$).

(after 24 h incubation). In cardiomyocytes, we also performed a time-dependent study with DOX and found that the effect on phospho-JNK and p38 occurred very early within 1 h of incubation with DOX (Fig. 10D). Taurine in the taurine + DOX group, however, prevented this DOX-induced activation of p38 and JNK.

3.13. Effects of JNK and p38 MAPK inhibition on DOX-induced apoptosis

We next investigated the effect of MAPK inhibition on DOX-induced apoptosis. We pre-treated cardiomyocytes with 10 μM SP600125 (a JNK inhibitor) and SB203580 (a p38 inhibitor) separately for 15 min for two different sets of experiments and then studied the effects of DOX and taurine on IKKα, IKKβ, NF-κB activation and cell viability. Both JNK and p38 inhibition significantly inhibited IKKα, IKKβ, NF-κB phosphorylation (Fig. 11A and B) in DOX-exposed cardiomyocytes and increased cell viability (Fig. 11C). There was a similar trend following taurine treatment, suggesting that taurine inhibits DOX-induced NF-κB phosphorylation and apoptosis by suppressing the activation of JNK and p38.

3.14. Potential protective mechanisms activated by taurine

We investigated the protective effect of taurine on DOX-induced cardiotoxicity by evaluating the phosphorylation patterns of Akt and PI3-K in DOX-induced cardiac pathophysiology. Doxorubicin significantly decreased Akt phosphorylation (Fig. 12A) and PI3-K protein levels (Fig. 12B), whereas taurine treatment maintained them at the levels seen in control animals. We next investigated the effect of PI3-K/Akt inhibition on DOX-induced apoptosis. PI3-K/Akt inhibition by LY294002 further reduced cardiomyocyte viability compared with doxorubicin alone (Fig. 12C). However, during taurine treatment without the inhibitor, cardiomyocyte viability was markedly enhanced. With the addition of the inhibitor, the protective effect of taurine was substantially reduced (Fig. 12C), indicating that the Akt activation pathway is protective against the progression of cardiac apoptosis.

3.15. Taurine phosphorylates Bad through PI3-K/Akt in cardiac myocytes

We subsequently examined the effect of taurine on Bad phosphorylation in cardiac myocytes. Fig. 13 shows that the protein content of phosphorylated Bad was decreased in DOX-treated cardiomyocytes. However, treatment with taurine increased Bad phosphorylation in DOX-treated cardiomyocytes (Fig. 13). Similarly, taurine by itself caused a significant increase in Bad phosphorylation. To test whether taurine induced Bad phosphorylation via a PI3-kinase/Akt dependent pathway, myocytes were preincubated with 10 μM LY294002 for 30 min before taurine treatment. LY294002 blocked the taurine-induced Bad phosphorylation in DOX-treated cells (Fig. 11). When Bad is phosphorylated, it becomes inactivated and prevented from binding to Bcl-2/Bcl-xL, thereby promoting cell survival.

3.16. Histological assessment

Fig. 14 illustrates the histological assessments of different cardiac segments of experimental animals. DOX injection caused disorganization of the normal radiating pattern of cell plates in the heart. Treatment with taurine reduced such changes, and the hearts appeared similar to that of normal.

4. Discussion

In the present study, we demonstrated that taurine provides dramatic recovery of rat heart and neonatal myocytes exposed to doxorubicin via the inactivation of p53 and JNK-p38. Additionally, taurine also increased Bad phosphorylation via the PI3Kinase/Akt signaling pathways. Thus, we propose that taurine mediates cardiomyocyte protection by regulating p53, JNK-p38 and increasing PI3Kinase/Akt activation.

Treatment of cancer patients with DOX might be responsible for the development of cardiomyopathy, which can lead to heart failure [53]. The data presented herein demonstrate that DOX administration increased the serum cardiotoxicity indices (LDH and CK), and this rise could cause heart failure [53]. The increase in serum cardiac enzyme content could be due to increased release after the doxorubicin-induced lipid peroxidation (oxidative stress) of cardiac membranes. However, we observed that this pathophysiological condition could be reversed upon taurine treatment. Oxidative stress due to increased ROS production plays a key role in the triggering and progression of DOX-induced myocardial dysfunction [9,10]. Intracellular GSH plays an important role in cellular defense against oxidative stress. Cardiac GSH depletion and the accumulation of its oxidized product, GSSG, occur during

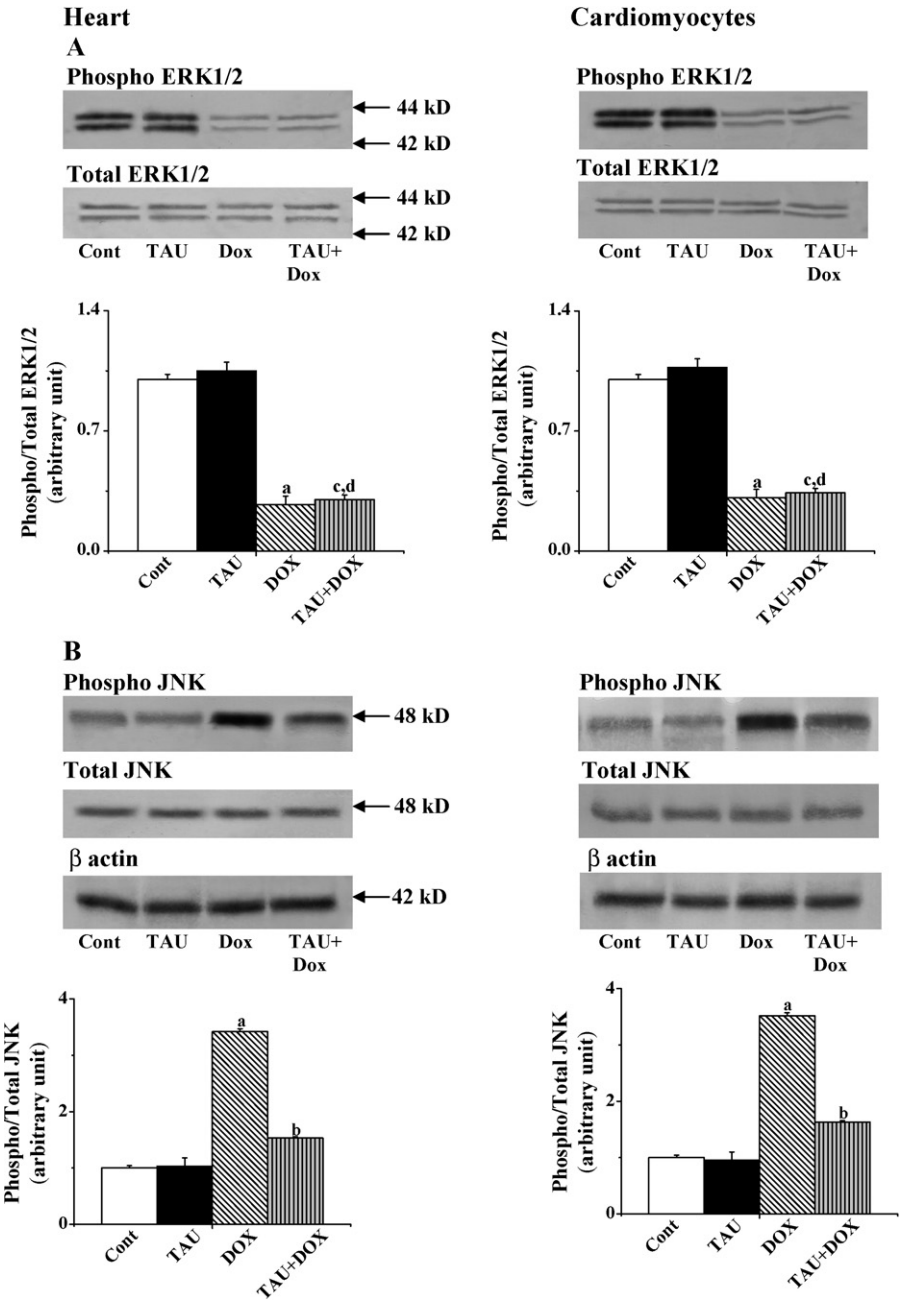

Fig. 10. Immunoblot analysis on MAPKinase family proteins in response to DOX and taurine (TAU + DOX). Panel A: Phospho and total ERK1/2, Panel B: phospho and total JNK, Panel C: phospho and total p38, Panel D: time dependent effect on JNK and p38 activation after DOX exposure in cardiomyocytes. β actin was used as an internal control. Data represent the average ± SD of 6 separate experiments in each group. "*a*" indicates the significant difference between the control and DOX-exposed groups, "*b*" indicates the significant difference between the DOX treated and taurine treated groups,"*c*" indicates the significant difference between the control and TAU + DOX treated cells, "*d*" indicates the significant difference between TAU and TAU + DOX treated cells. ($P^a < 0.05$, $P^b < 0.05$, $P^c < 0.05$, $P^d < 0.05$).

oxidative stress caused by increased cellular demand and lead to impaired cell function [54,55]. In DOX-treated hearts, we observed increased oxidative damage, as shown by markedly increased lipid peroxidation products (MDA), depleted GSH (and increase in GSSG) levels and decreased antioxidant enzyme activities. However, taurine supplementation effectively reduced these alterations in DOX-induced cardiac pathophysiology.

DOX-induced mitochondrion-dependent apoptotic death of cardiomyocytes is the most direct cause of DOX cardiotoxicity. In this pathophysiology, pro-apoptotic Bcl-2 members, mitochondrial effectors and caspases are activated to provoke apoptotic cell death [11]. DOX-induced extrinsic receptor-mediated and the ER/SR pathways are also known for inducing apoptotic cell death [56]. In the present study, we observed that DOX induced apoptosis (confirmed by flow cytometry and DNA fragmentation analyses), up-regulated pro-apoptotic (Bad, Bax) and down-regulated anti-apoptotic (Bcl-2, Bcl-xL) proteins, reduced mitochondrial membrane potential, increased cytochrome c release into the cytosol and the cleavage of caspases 9 and 3 and PARP in cardiomyocytes. Additionally, DOX significantly increased intracellular Ca^{2+} concentrations and activated caspase-12, an ER/SR stress-associated caspase. The increased intracellular Ca^{2+} can in turn induce ROS production through Ca^{2+}-sensitive ROS-generating enzymes and the increased ROS production further releases Ca^{2+} from the

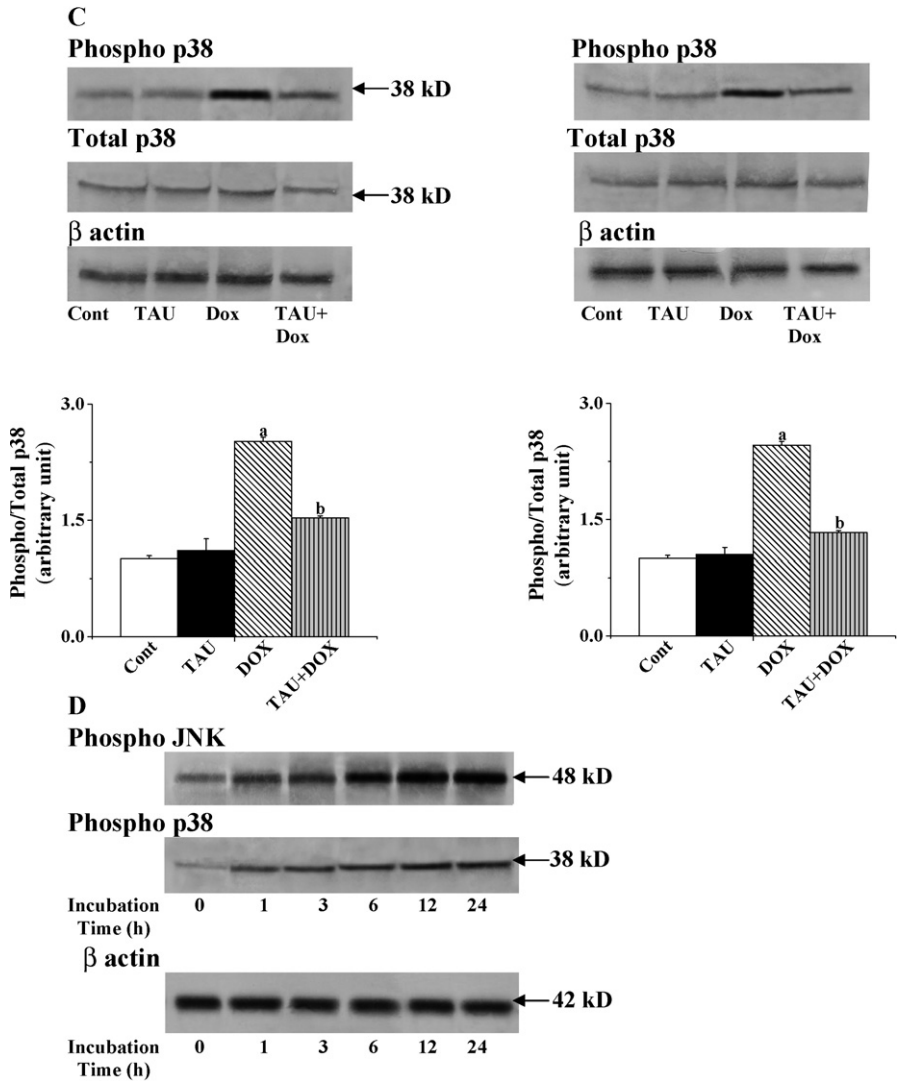

Fig. 10. (*Continued*).

sarcoplasmic reticulum [57]. However, Liu et al. [11] demonstrated that the extrinsic receptor-mediated pathway was not activated at the dose of DOX used in the present study. Thus, DOX could activate the mitochondrial and ER/SR-mediated apoptotic signal transduction pathways in cardiomyocytes under the present pathophysiological conditions. However, taurine could antagonize all of these DOX-mediated pro-apoptotic events.

Numerous studies have shown that DOX-induced apoptotic death of cardiomyocytes is associated with increased expression of p53 tumor suppressor protein [11] in response to both DNA damage and oxidative stress. Once activated, it up-regulates the downstream gene Bax and thereby activates the intrinsic apoptotic pathway [58]. In the present study, we observed that p53 expression was increased in both hearts and cardiomyocytes exposed to DOX. However, taurine modulated this activation of p53.

One of the major signal-transduction pathways activated in response to oxidative stress is the NF-κB pathway [59,60]. Its activation might either promote or block cell death, depending upon the cell types and the nature of oxidative stimuli used in a particular study [61,62]. Our results showed that DOX exposure induced NF-κB phosphorylation in cardiomyocytes, suggesting that NF-κB activation is pro-apoptotic in DOX-induced myocardial injury. Our findings also indicated that DOX activates NF-κB through a mechanism that requires IκBα phosphorylation, as evidenced by Western blot analysis. Moreover, when cardiomyocytes were pre-exposed to PS-1145, a specific IKK inhibitor, caspase-3 activation and PARP cleavage were not observed, indicating that DOX induces cardiomyocyte apoptosis by activating nuclear factor κB. However, taurine protected cardiomyocytes from apoptosis by inhibiting NF-κB activation.

It is well known that MAPKs play important roles in cell proliferation, differentiation and death. These kinases are also involved in the response to ROS-induced oxidative stress. In the present study, we therefore studied the effects of DOX and taurine on MAPK (ERK, JNK, and p38-MAPK) signaling pathways by immunoblot analysis to further investigate the effects of taurine on the inhibition of apoptosis. DOX exposure significantly increased the phosphorylation of JNK and p38, whereas the phosphorylation of ERK in both rat hearts and cardiomyocytes was decreased. In addition, a specific inhibitor of JNK, SP600125, or a specific inhibitor of p38, SB203580, suppressed DOX-induced NF-κB activation. Thus, decreased NF-κB activity by these specific inhibitors strongly indicates the involvement of JNK and p38 MAPK in DOX-induced NF-κB activation. However, taurine prevented these DOX-induced changes in JNK and p38 phosphorylation, thereby blocking NF-κB activation and apoptosis.

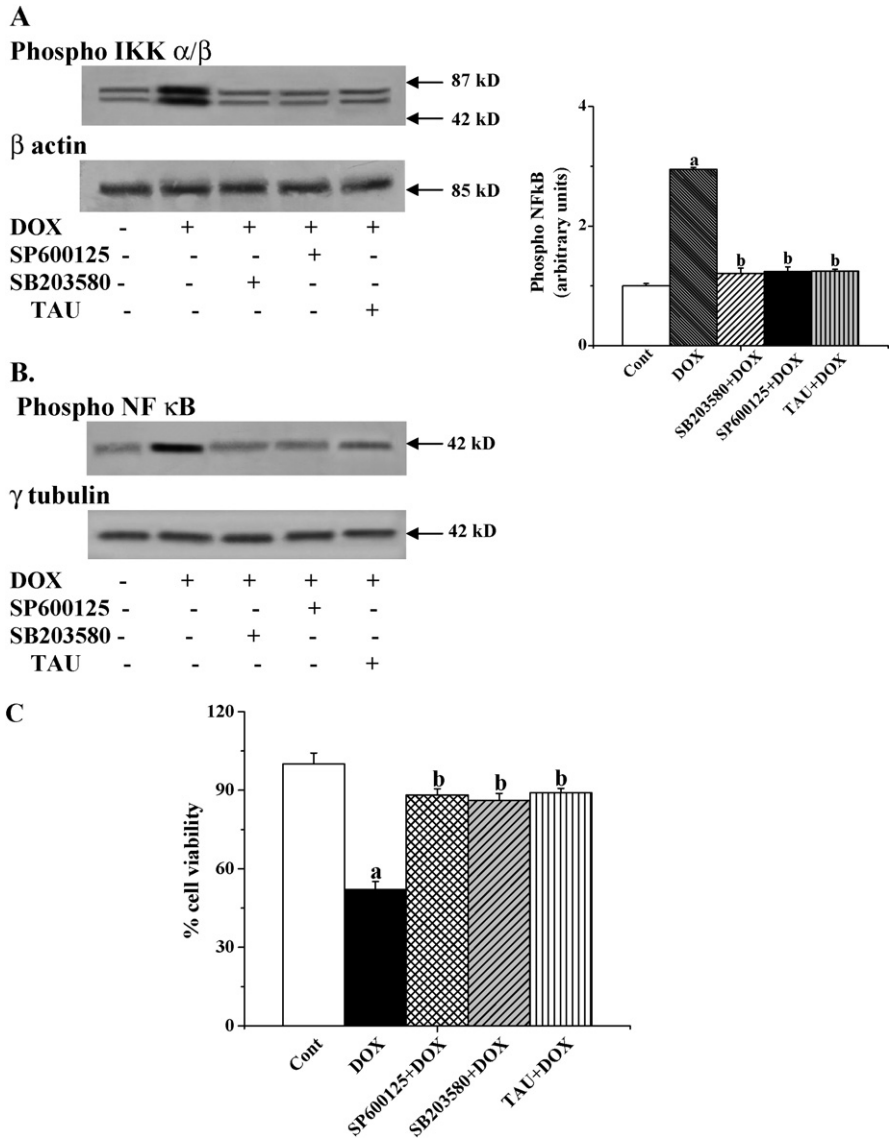

Fig. 11. Immunoblot analysis of IKKα/β, NFκB and cardiomyocytes viability in response to SB203580 and SP600125. Cardiomyocytes were pre-treated with 10 μM SB203580 and SP600125 for 15 min, then treated with DOX (1 μM), taurine (25 mM, added 1 h prior to DOX treatment) for 24 h. Panel A: phospho IKKα/β, β actin was used as an internal control. Panel B: phospho NFκB, γ tubulin was used as an internal control. Panel C: effects of SP600125 and SB203580 on cell viability. Data represent the average ± SD of 6 separate experiments in each group. "*a*" indicates the significant difference between the control and DOX-exposed groups, "*b*" indicates the significant difference between the DOX treated and taurine/SP600125/SB203580 treated groups.($P^a < 0.05$, $P^b < 0.05$).

A large number of studies have shown that the PI 3-kinase/Akt signaling pathway provides an important cell survival signal in cardiomyocytes [39–43]. In our present study, PI 3-kinase and p-Akt levels were reduced in DOX-exposed rat hearts and cardiomyocytes compared with the control groups. Similarly, DOX exposure also reduced Bad phosphorylation in cardiomyocytes. These alterations in PI 3-kinase, phosphorylated Akt and phosphorylated Bad due to DOX exposure were attenuated by treatment with taurine because of either increased synthesis or less degradation of these proteins in the presence of taurine. Studies with the PI3-K/Akt specific inhibitor LY294002 showed that it could block taurine-induced Bad phosphorylation and that it reduced cell viability in DOX-treated cardiomyocytes. This observation indicates that taurine induced Bad phosphorylation, thereby conferring protection against DOX via a PI 3-kinase/Akt-dependent pathway.

The sulfur-containing β-amino acid taurine (2-aminoethanesulfonic acid) is found in relatively high concentrations in the heart compared with other organs, at approximately 25% in humans and 50% in rodents. In addition, taurine is neither metabolized nor incorporated into cellular proteins in mammals, suggesting an important requirement for free cytosolic taurine in the normal physiology [29,63]. Because taurine possesses potent antioxidant properties in various pathophysiological states [64–68], its depletion causes severe cardiomyopathy and heart failure [69,70]. Therefore, myocardial taurine levels should be increased with the help of external agents (like taurine) to protect the cardiovascular system from DOX exposure. In the present study, we observed that the cardiac taurine level was decreased in DOX-exposed rats, whereas treatment with taurine significantly increased its level in cardiac tissue.

In conclusion, the present study has demonstrated the mechanism of action of the protective role of taurine against doxorubicin-induced cardiac oxidative stress. This in vivo and in vitro study clearly showed that doxorubicin impaired cardiac cell survival at least partially through the activation of p53 and JNK-p38, which

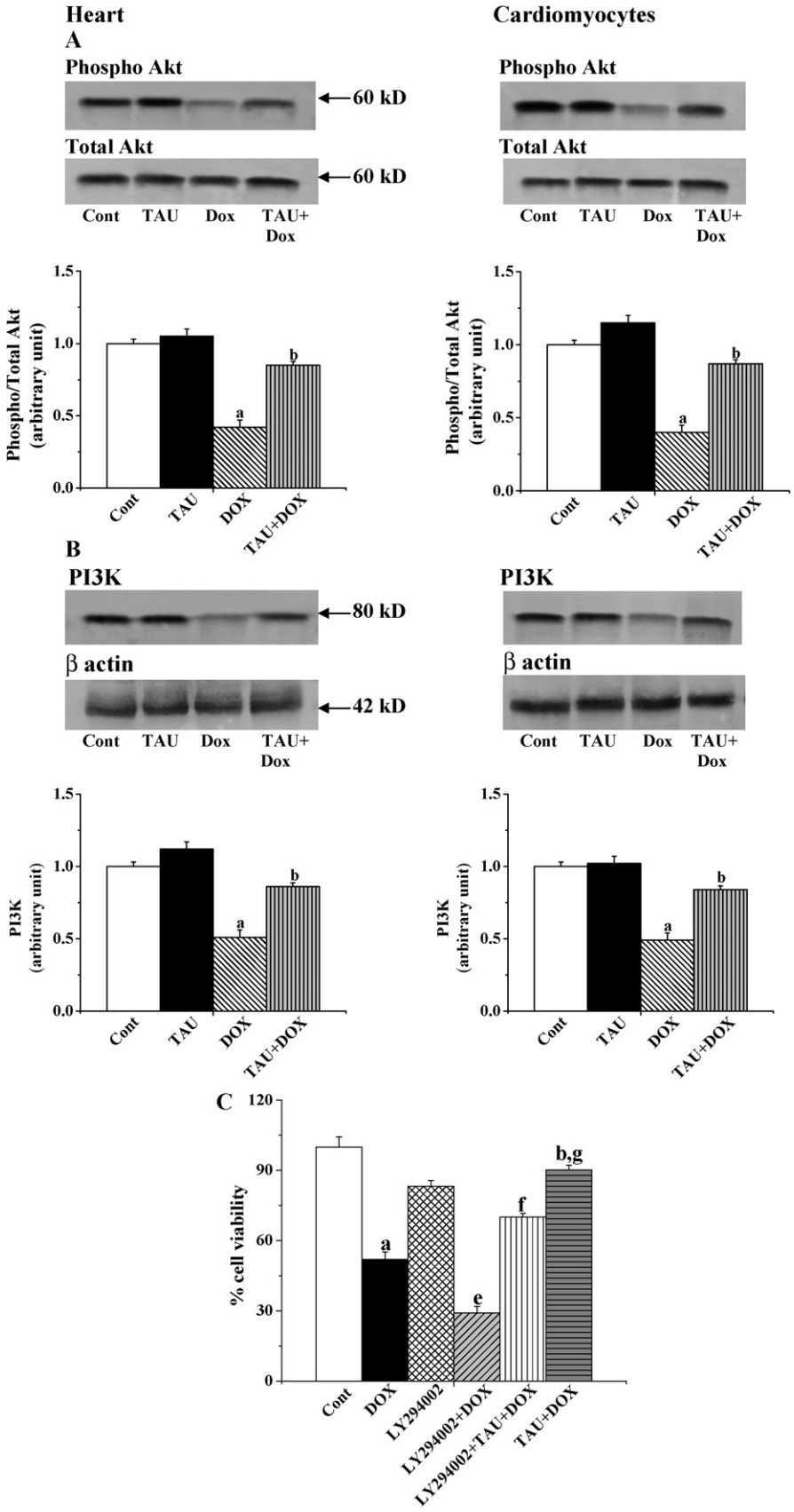

Fig. 12. Immunoblot analysis of AKT, PI3-K and cell viability in response to taurine and LY294002. Cardiomyocytes were pre-treated with 10 μM LY294002 for 30 min, then treated with DOX (1 μM), taurine (25 mM, added 1 h prior to DOX treatment) for 24 h. Panel A: phospho and total AKT, Panel B: PI3-K, β actin was used as an internal control. Panel C: effect of LY294002 on cell viability. Data represent the average ± SD of 6 separate experiments in each group. "*a*" indicates the significant difference between the control and DOX-exposed groups, "*b*" indicates the significant difference between the DOX treated and taurine treated groups, "*e*" indicates the significant difference between the DOX treated and LY294002 + DOX treated groups, "*f*" indicates the significant difference between the LY294002 + DOX treated and LY294002 + DOX + TAU treated groups and "*g*" indicates the significant difference between the LY294002 + DOX + TAU treated and TAU + DOX treated groups. ($P^a < 0.05$, $P^b < 0.05$, $P^e < 0.05$, $P^f < 0.05$, $P^g < 0.05$).

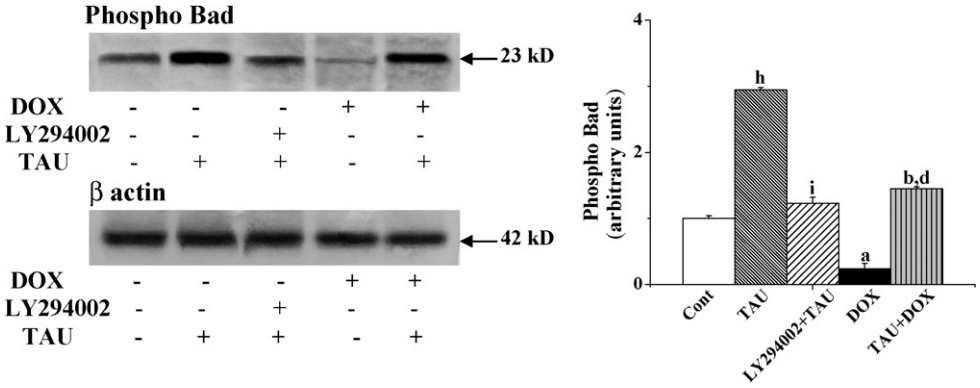

Fig. 13. Immunoblot analysis of phosphorylation of Bad in response to LY294002 and taurine. Cardiomyocytes were pre-treated with 10 μM LY294002 for 30 min, then treated with DOX (1 μM), taurine (25 mM, added 1 h prior to DOX treatment) for 24 h. Data represent the average ± SD of 6 separate experiments in each group. "*a*" indicates the significant difference between the control, DOX-exposed groups, "*b*" indicates the significant difference between the DOX treated and taurine treated groups, "*d*" indicates the significant difference between TAU and TAU + DOX treated cells. "*h*" indicates the significant difference between the control and TAU treated groups, "*i*" indicates the significant difference between the TAU treated and LY294002 + TAU treated groups.($P^a < 0.05$, $P^b < 0.05$, $P^d < 0.05$, $P^h < 0.05$, $P^i < 0.05$).

ultimately led to NF-κB activation via the IKK pathway and mitochondrion-dependent cell apoptosis. Taurine treatment ameliorated nearly all of these apoptotic actions of doxorubicin via the inhibition of the p53- and JNK-p38-dependent pathways and up-regulation of PI3-K/Akt phosphorylation (as indicated in the proposed scheme of Fig. 15). These impressive benefits and the absence of toxicity with taurine supplementation may provide clues to understanding the cardiac protective mechanism of taurine. We, therefore, propose that increased dietary taurine intake represents an important nutritional modification that may provide a useful intervention to reduce the worldwide burden from doxorubicin-induced cardiovascular disease.

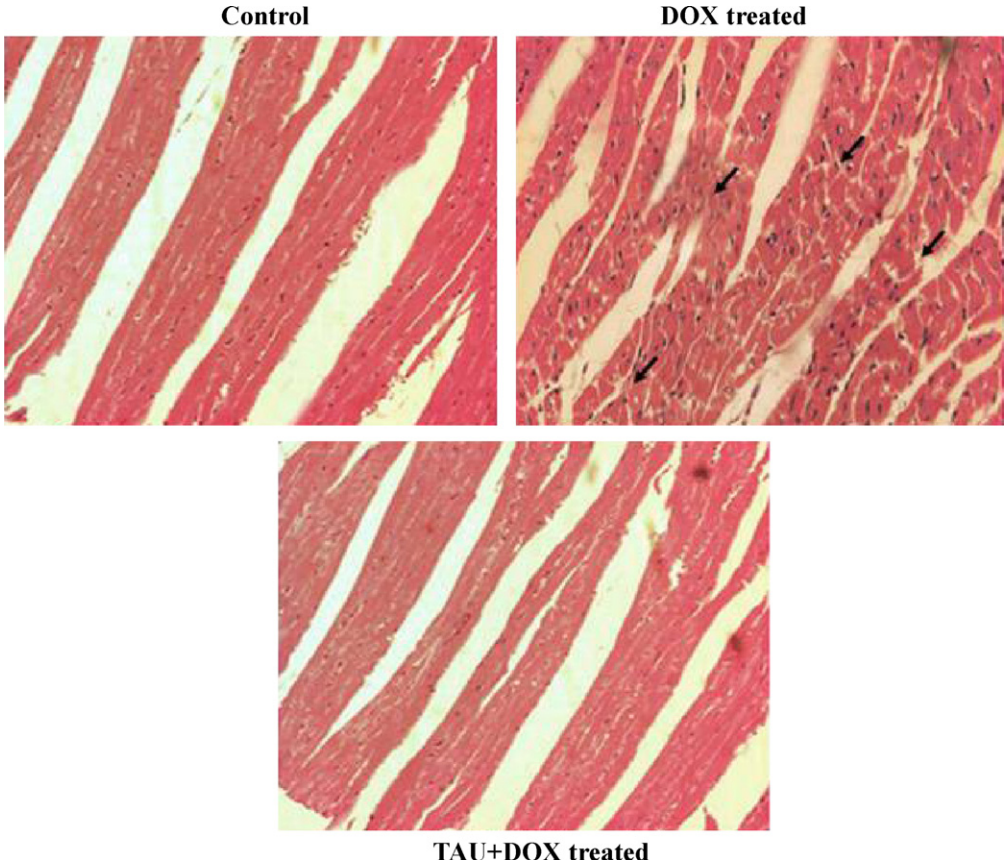

Fig. 14. Haematoxylin and eosin stained cardiac section of normal, DOX and taurine-treated rats (10×). Arrows indicate disorganization of normal radiating pattern of cell plates in the heart in DOX-exposed animals.

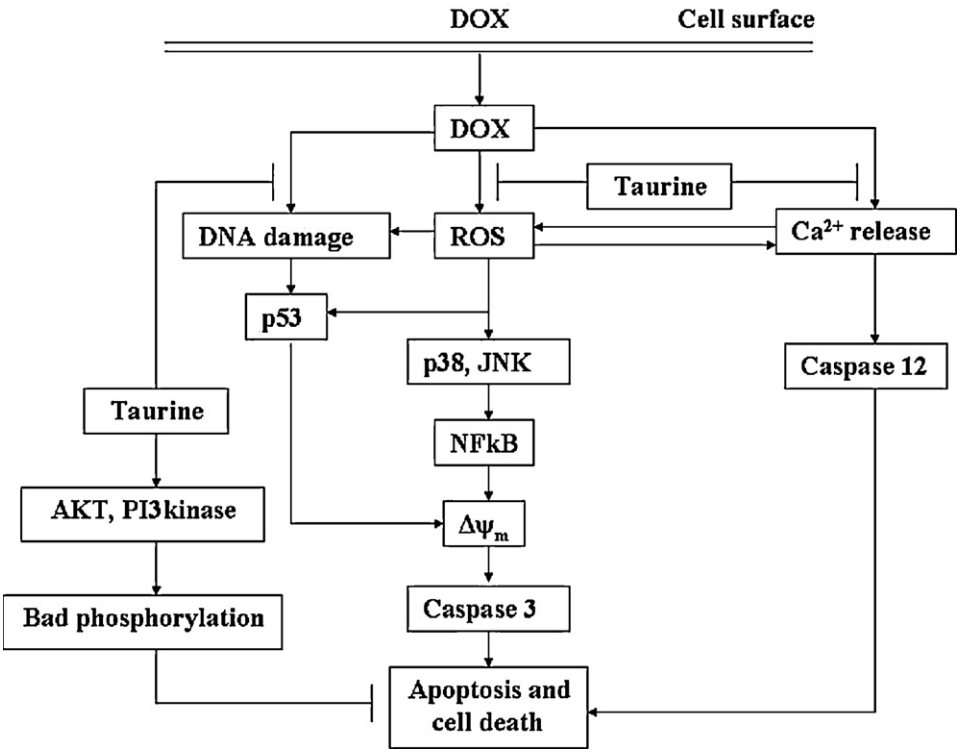

Fig. 15. Schematic diagram of the DOX induced cardiotoxicity and its prevention by taurine.

Acknowledgement

The authors are grateful to Mr. Prasanta Pal for excellent technical assistance for the study.

References

[1] Hortobagyi GN. Anthracyclines in the treatment of cancer. An overview. Drugs 1997;54(Suppl.):1–7.
[2] Lown JW. Anthracycline and anthraquinone anticancer agents: current status and recent developments. Pharmacol Ther 1993;60:185–214.
[3] Orhan B. Doxorubicin cardiotoxicity: growing importance. J Clin Oncol 1999;17:2294–6.
[4] Silber JH, Barber G. Doxorubicin-induced cardiotoxicity. N Engl JMed 1995;333:1359–60.
[5] Iliskovic N, Singal PK. Lipid lowering: an important factor in preventing adriamycin-induced heart failure. Am J Pathol 1997;150:727–34.
[6] Valdes Olmos RA, Ten Bokkel Huinink WW, Ten Hoeve RF, Van Tinteren H, Bruning PF, Van Vlies B. Assessment of anthracycline-related myocardial adrenergic derangement by [123I]metaiodobenzylguanidine scintigraphy. Eur J Cancer 1995;31:26–31.
[7] Wang YX, Korth M. Effects of doxorubicin on excitation–contraction coupling in guinea pig ventricular myocardium. Circ Res 1995;76:645–53.
[8] Torre-Amione G, Kapadia S, Benedict C, Oral H, Young JB, Mann DL. Proinflammatory cytokine levels in patients with depressed left ventricular ejection fraction: a report from the Studies of Left Ventricular Dysfunction (SOLVD). J Am Coll Cardiol 1996;27:1201–6.
[9] Arola OJ, Saraste A, Pulkki K, Kallajoki M, Parvinen M, Voipio- Pulkki LM. Acute doxorubicin cardiotoxicity involves cardiomyocyte apoptosis. Cancer Res 2000;60:1789–92.
[10] Childs AC, Phaneuf SL, Dirks AJ, Phillips T, Leeuwenburgh C. Doxorubicin treatment in vivo causes cytochrome C release and cardiomyocyte apoptosis, as well as increased mitochondrial efficiency, superoxide dismutase activity, and Bcl-2:Bax ratio. Cancer Res 2002;62:4592–8.
[11] Liu TJ, Yeh YC, Ting CT, Lee WL, Wang LC, Lee HW, et al. Ginkgo biloba extract 761 reduces doxorubicin-induced apoptotic damage in rat hearts and neonatal cardiomyocytes. Cardiovasc Res 2008;80:227–35.
[12] Nakamura T, Ueda Y, Juan Y, Katsuda S, Takahashi H, Koh E. Fas-mediated apoptosis in adriamycin-induced cardiomyopathy in rats: in vivo study. Circulation 2000;102:572–8.
[13] Tsang WP, Chau SPY, Kong SK, Fung KP, Kwok TT. Reactive oxygen species mediate doxobubicin induced p53-independent apoptosis. Life Sci 2003;73:2047–58.
[14] Wang Y, Su B, Sah VP, Brown JH, Han J, Chien KR. Cardiac hypertrophy induced by mitogen-activated protein kinase kinase 7, a specific activator for c-Jun NH2-terminal kinase in ventricular muscle cells. J Biol Chem 1998;273:5423–6.
[15] Kyriakis JM, Avruch J. Sounding the alarm: protein kinase cascades activated by stress and inflammation. J Biol Chem 1996;271:24313–6.
[16] Wang X, Martindale JL, Liu Y, Holbrook NJ. The cellular response to oxidative stress: influences of mitogen-activated protein kinase signalling pathways on cell survival. Biochem J 1998;333:291–300.
[17] Kim SB, Kim JS, Lee JH, Yoon WJ, Lee DS, Ko MS, et al. NF-kB activation is required for cisplatin-induced apoptosis in head and neck squamous carcinoma cells. FEBS Lett 2006;580:311–8.
[18] Chong ZZ, Li F, Maiese K. Erythropoietin requires NF-kB and its nuclear translocation to prevent early and late apoptotic neuronal injury during beta-amyloid toxicity. Curr Neurovasc Res 2005;2:387–99.
[19] Lou H, Danelisen I, Singal PK. Involvement of mitogen-activated protein kinases in adriamycin-induced cardiomyopathy. Am J Physiol Heart Circ Physiol 2005;288:1925–30.
[20] Li S, Yu B. Adriamycin induces myocardium apoptosis through activation of nuclear factor kB in rat. Mol Biol Rep 2008;35:489–94.
[21] Birdsall TC. Therapeutic applications of taurine. Altern Med Rev 1998;3:128–36.
[22] Sakaguchi M, Murata M. Seasonal variations of free amino acids in oyster whole body and adductor muscle. Nippon Suisan Gakkaishi 1989;55:2037–41.
[23] Chesney RW. Taurine: Its biological role and clinical implications. Adv Pediatr 1985;32:1–42.
[24] Das J, Ghosh J, Manna P, Sil PC. Protective role of taurine against arsenic-induced mitochondria-dependent hepatic apoptosis via the inhibition of PKCδ-JNK pathway. PLoS ONE 2010;5:1–19. e12602.
[25] Das J, Ghosh J, Manna P, Sil PC. Acetaminophen induced acute liver failure via oxidative stress and JNK activation: protective role of taurine by the suppression of cytochrome P450 2E1. Free Radic Res 2010;44:340–55.
[26] Manna P, Sinha M, Sil PC. Taurine plays a beneficial role against cadmium-induced oxidative renal dysfunction. Amino Acids 2009;36:417–28.
[27] Manna P, Sinha M, Sil PC. Taurine triggers a chemoprevention against cadmium induced testicular oxidative injury. Reprod Toxicol 2008;26:282–91.
[28] Sinha M, Manna P, Sil PC. Cadmium induced neurological disorders: prophylactic role of taurine. J Appl Toxicol 2008;28:974–86.
[29] Huxtable RJ. Physiological actions of taurine. Physiol Rev 1992;72:101–63.
[30] Redmond HP, Wang JH, Bouchier-Hayes D. Taurine attenuates nitric oxide and reactive oxygen intermediate-dependent hepatocyte injury. Arch Surg 1996;131:1280–7.
[31] Kontny E, Szczepanska K, Kowalczewski J, Kurowska M, Janicka I, Marcinkiewicz J, et al. The mechanism of taurine chloramine inhibition of cytokine

(interleukin-6, interleukin-8) production by rheumatoid arthritis fibroblast-like synoviocytes. Arthritis Rheum 2000;43:2169–77.
[32] Haunstetter A, Izumo S. Apoptosis: basic mechanisms and implications for cardiovascular disease. Circ Res 1998;82:1111–29.
[33] Hsu TC, Chiang SY, Wu JH, Tsai CC, Huang CY, Chen YC, et al. Treatment with taurine attenuates hepatic apoptosis in NZB/W F1 mice fed with a high-cholesterol diet. J Agric Food Chem 2008;56:9685–91.
[34] Racasan S, Braam B, van der Giezen DM, Goldschmeding R, Boer P, Koomans H. A. Perinatal L-arginine and antioxidant supplements reduce adult blood pressure in spontaneously hypertensive rats. Hypertension 2004;44:83–8.
[35] Harada H, Cusack BJ, Olson RD, Stroo W, Azuma J, Hamaguchi T, et al. Taurine deficiency and doxorubic pump. Biochem Pharmacol 1990;39:745–51.
[36] Hamaguchi T, Azuma J, Awata N, Ohta H, Takihara K, Harada H, et al. Reduction of doxorubicin-induced cardiotoxicity in mice by taurine. Res Commun Chem Pathol Pharmacol 1988;59:21–30.
[37] Ito T, Muraoka S, Takahashi K, Fujio Y, Schaffer SW, Azuma J. Beneficial effect of taurine treatment against doxorubicin-induced cardiotoxicity in mice. Adv Exp Med Biol 2009;643:65–74.
[38] Huang XM, Zhu WH, Kang ML. Study on the effect of doxorubicin on expressions of genes encoding myocardial sarcoplasmic reticulum Ca^{2+} transport proteins and the effect of taurine on myocardial protection in rabbits. J Zhejiang Univ Sci 2003;4:114–20.
[39] Wang Y. Mitogen-activated protein kinases in heart development and diseases. Circulation 2007;116:1413–23.
[40] Yellon DM, Hausenloy DJ. Myocardial reperfusion injury. N Engl JMed 2007;357:1121–35.
[41] Ahmed NN, Grimes HL, Bellacosa A, Chan TO, Tsichlis PN. Transduction of interleukin-2 antiapoptotic and proliferative signals via Akt protein kinase. Proc Natl Acad Sci USA 1997;94:3627–32.
[42] Yao R, Cooper GM. Requirement for phosphatidylinositol-3 kinase in the prevention of apoptosis by nerve growth factor. Science 1995;267:2003–6.
[43] Yin H, Chao L, Chao J. Kallikrein/kinin protects against myocardial apoptosis after ischemia/reperfusion via Akt glycogen synthase kinase-3 and Akt-bad-14-3-3 signaling pathways. J Biol Chem 2005;280:8022–30.
[44] Jahnukainen K, Jahnukainen T, Salmi TT, Svechnikov K, Eksborg S, Soder O. Amifostine protects against early but not late toxic effects of doxorubicin in infant rats. Cancer Res 2001;61:6423–7.
[45] Bradford MM. A rapid and sensitive method for the quantitation of microgram quantities of protein utilizing the principle of protein–dye binding. Anal Biochem 1976;72:248–54.
[46] Esterbauer H, Cheeseman KH. Determination of aldehydic lipid peroxidation products: malonaldehyde and 4-hydroxynonenal. Methods Enzymol 1990;186:407–21.
[47] Kornberg A. Lactic dehydrogenase of muscle. In: Colowick SP, Kaplan NO, editors. Methods enzymol. New York: Academic press; 1955. p. 441–3.
[48] Das J, Ghosh J, Manna P, Sinha M, Sil PC. Taurine protects rat testes against $NaAsO_2$-induced oxidative stress and apoptosis via mitochondrial dependent and independent pathways. Toxicol Lett 2009;187:201–10.
[49] Ferreira MPLV0, Nunes MV, Mendes E, Remiilo F, Ferreirat IMA. Development of an HPLC–UV method for determination of taurine in infant formulae and breast milk. J Liq Chrom Rel Technol 1997;20:1269–78.
[50] Sil P, Kandaswamy V, Sen S, Increased protein kinase C activity in myotrophin-induced myocyte growth. Circ Res 1998;82:1173–88.
[51] Sellins KS, Cohen JJ. Gene induction by gamma-irradiation leads to DNA fragmentation in lymphocytes. J Immunol 1987;139:3199–206.
[52] Goren N, Cuenca J, Martín-Sanz P, Bosca L. Attenuation of NF-kB signalling in rat cardiomyocytes at birth restricts the induction of inflammatory genes. Cardiovasc Res 2004;64:289–97.
[53] Lefrak EA, Pitha J, Rosenheim S, Gottlieb JA. Clinicopathologic analysis of adriamycin cardiotoxicity. Cancer 1973;32:302–14.
[54] Forgione MA, Cap A, Liao R, Moldovan NI, Eberhardt RT, Lim CC, et al. Heterozygous cellular glutathione peroxidase deficiency in the mouse: abnormalities in vascular and cardiac function and structure. Circulation 2002;106:1154–8.
[55] Li S, Li X, Rozanski GJ. Regulation of glutathione in cardiac myocytes. J Mol Cell Cardiol 2003;35:1145–52.
[56] Chua CC, Liu X, Gao J, Hamdy RC, Chua BHL. Multiple actions of pifithrin-α on doxorubicin-induced apoptosis in rat myoblastic H9c2 cells. Am J Physiol Heart Circ Physiol 2006;90:2606–13.
[57] Kim SY, Kim SJ, Kim BJ, Rah SY, Chung SM, Im MJ, et al. Doxorubicin-induced reactive oxygen species generation and intracellular Ca^{2+} increase are reciprocally modulated in rat cardiomyocytes. Exp Mol Med 2006;38:535–45.
[58] Liu X, Chua CC, Gao J, Chen Z, Landy CL, Hamdy R, et al. Pifithrin-alpha protects against doxorubicin-induced apoptosis and acute cardiotoxicity in mice. Am J Physiol Heart Circ Physiol 2004;286:933–9.
[59] Baeuerle PA, Henkel T. Function and activation of NF-kB in the immune system. Annu Rev Immunol 1994;12:141–79.
[60] Chen F, Castranova V, Shi X, Demers LM. New insights into the role of nuclear factor-kB, a ubiquitous transcription factor in the initiation of diseases. Clin Chem 1999;45:7–17.
[61] Boland MP, Foster SJ, O'Neill LAJ. Daunorubicin activates NFkB and induces kB-dependent gene expression in HL-60 promyelocytic and Jurkat T lymphoma cells. J Biol Chem 1997;272:12952–60.
[62] Aoki M, Nata T, Morishita R, Matsushita H, Nakagami H, Yamamoto K, et al. Endothelial apoptosis induced by oxidative stress through activation of NF-kB: antiapoptotic effect of antioxidant agents on endothelial cells. Hypertension 2001;38:48–55.
[63] Sole MJ, Jeejeebhoy KN. Conditioned nutritional requirements and the pathogenesis and treatment of myocardial failure. Curr Opin Clin Nutr Metab Care 2000;3:417–24.
[64] Das J, Ghosh J, Manna P, Sil PC. Taurine protects acetaminophen-induced oxidative damage in mice kidney through APAP urinary excretion and CYP2E1 inactivation. Toxicology 2010;269:24–34.
[65] Ghosh J, Das J, Manna P, Sil PC. Taurine prevents arsenic-induced cardiac oxidative stress and apoptotic damage: role of NF-κB, p38 and JNK MAPK pathway. Toxicol Appl Pharm 2009;240:73–87.
[66] Das J, Ghosh J, Manna P, Sinha M, Sil PC. Arsenic-induced oxidative cerebral disorders: protection by taurine. Drug Chem Toxicol 2009;32:93–102.
[67] Roy A, Manna P, Sil PC. Prophylactic role of taurine on arsenic mediated oxidative renal dysfunction via MAPKs/NF-kappaB and mitochondria dependent pathways. Free Radical Res 2009;43:995–1007.
[68] Manna P, Sinha M, Sil PC. Amelioration of cadmium-induced cardiac impairment by taurine. Chem Biol Interact 2008;174:88–97.
[69] Pion PD, Kittleson MD, Rogers QR, Morris JG. Myocardial failure in cats associated with low plasma taurine: a reversible cardiomyopathy. Science 1987;237:764–8.
[70] Moise NS, Pacioretty LM, Kallfelz FA, Stipanuk MH, King JM, Gilmour RF. Dietary taurine deficiency and dilated cardiomyopathy in the fox. Am Heart J 1991;121:541–7.